

8
NUREG/CR-4489

EGG-2436

March 1986

Venting of Noncondensable Gas From the Upper Head of a B&W Reactor Vessel Using Hot Leg U-Bend Vent Valves

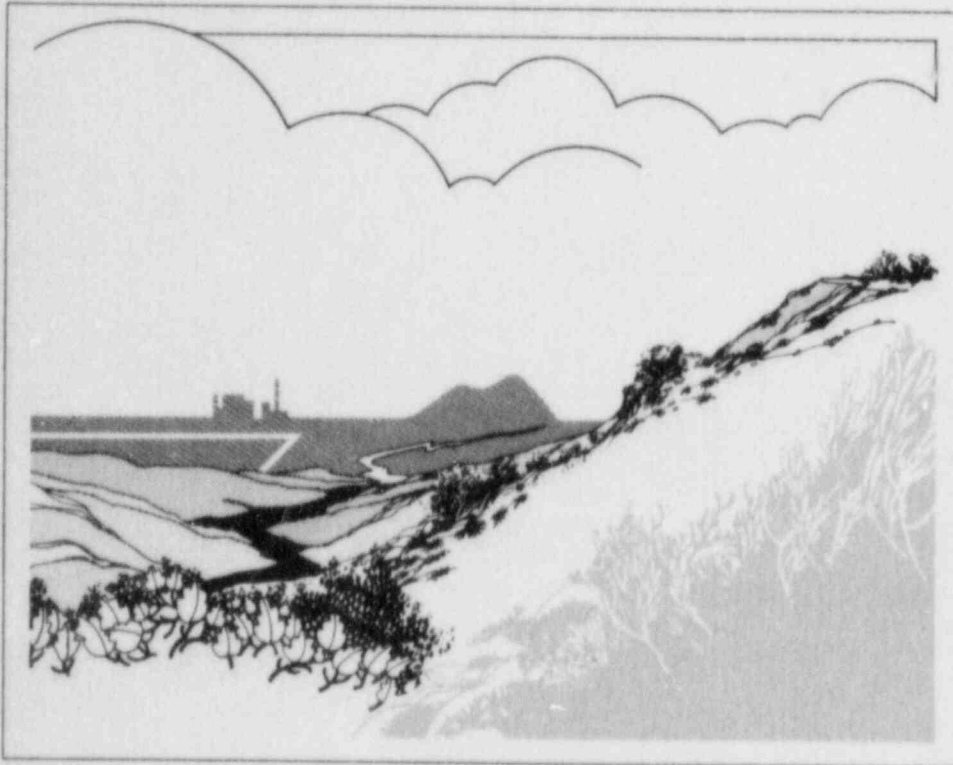
Michael E. Waterman
Craig M. Kullberg
Philip D. Wheatley

F O R M A L R E P O R T



Work performed under
DOE Contract No. DE-AC07-76ID01570

for the **U.S. Nuclear
Regulatory Commission**



Idaho National Engineering Laboratory

Managed by the U.S. Department of Energy

8605290063 860331
PDR NUREG
CR-4488 R PDR

Available from

Superintendent of Documents
U.S. Government Printing Office
Post Office Box 37082
Washington, D.C. 20013-7982

and

National Technical Information Service
Springfield, VA 22161

NOTICE

This report was prepared as an account of work sponsored by an agency of the United States Government. Neither the United States Government nor any agency thereof, nor any of their employees, makes any warranty, expressed or implied, or assumes any legal liability or responsibility for any third party's use, or the results of such use, of any information, apparatus, product or process disclosed in this report, or represents that its use by such third party would not infringe privately owned rights.

NUREG/CR-4489
EGG-2436
Distribution Category: R4

**VENTING OF NONCONDENSIBLE GAS
FROM THE UPPER HEAD OF
A B&W REACTOR VESSEL USING
HOT LEG U-BEND VENT VALVES**

Michael E. Waterman
Craig M. Kullberg
Philip D. Wheatley

Published March 1986

**EG&G Idaho, Inc.
Idaho National Engineering Laboratory
Idaho Falls, Idaho 83415**

Prepared for the
U.S. Nuclear Regulatory Commission
Division of Nuclear Reactor Regulation
Office of Nuclear Regulatory Research
Washington, D.C. 20555
Under DOE Contract No. DE-AC07-76ID01570
FIN No. A6825

ABSTRACT

This report describes RELAP5/MOD2 thermal-hydraulic analyses of noncondensable gas removal from Babcock and Wilcox (B&W) reactor systems before and during natural circulation conditions following a severe core damage accident. Hot leg U-bend vent valves were modeled as the principal noncondensable venting pathway. The analyses will assist the U.S. Nuclear Regulatory Commission (NRC) in determining whether three B&W plants should receive permanent exemptions from a reactor vessel upper head vent requirement.

The raised-loop plant analysis was conducted to determine the effect of a reactor vessel upper head vent line on plant refill and recovery of natural circulation. The lowered-loop plant analysis investigated the removal of noncondensable gas during natural circulation.

The raised-loop calculations were started prior to recovery of natural circulation. The upper head vent line was connected to the steam generator inlet plenum of the loop without the pressurizer. In the case without the reactor vessel vent line, the loop with the pressurizer refilled 370 s sooner than the loop without the pressurizer. The reactor vessel vent line did not prevent the refilling of the primary system, but the refilling time was 520 s longer with the vent line than without the vent line. Consequently, since the loop with the pressurizer fills faster and the vent line delays refilling, the vent line should be connected to the loop with the pressurizer. In both simulations, at least 85% of the noncondensable mass was removed within the first hour.

The lowered-loop analysis investigated noncondensable gas removal during natural circulation. Approximately 20% of the original noncondensable inventory was removed in 2400 s. The removal rate was approximately one percent per hundred seconds after the initial removal period. The analysis indicates that 59% of the original inventory could be removed in approximately 6900 s. The method of removal appears to produce brief periods of natural circulation interruption (100 s) during which the removal rates are most significant.

In both the raised-loop and lowered-loop analyses, significant amounts of noncondensable gas were removed. Additionally, no fuel rod cladding temperature increases were predicted during the periods of loop stagnation.

SUMMARY

The U.S. Nuclear Regulatory Commission (NRC) requires installation of remotely operated reactor vessel head vents for noncondensable gas removal during transients. The vessel head vent removes noncondensable gases from the primary coolant system which might otherwise inhibit core cooling during natural circulation.

Three Babcock and Wilcox (B&W) plants (Davis-Besse, Crystal River, and Rancho Seco) have received temporary exemptions based on preliminary studies. The licensees for these plants contend that noncondensable gas in the reactor vessel upper head will not affect core cooling. Additionally, they contend that the vents in the reactor coolant system hot legs could remove the noncondensable gases without loss of natural circulation.

The Davis-Besse raised-loop plant licensee proposes the installation of a line connecting the reactor vessel upper head to the steam generator inlet on the loop with the pressurizer. The licensee concludes this design provides for continuous flow through the reactor vessel head and thereby retards steam formation in the reactor vessel head during natural circulation cooldown. Additionally, the licensee maintains that this arrangement will allow for the timely venting of noncondensable gases from the reactor vessel upper head without adversely affecting the time needed to refill the primary system and recover natural circulation. Nevertheless, the NRC is concerned that the flow of gas to a steam generator might retard decay heat removal.

RELAP5/MOD2 was used to estimate noncondensable gas removal by the hot leg high point vent valves (HPVVs) and power-operated relief valve (PORV) before and during natural circulation conditions. The pre-natural circulation analysis evaluated the time required to refill the primary system of a raised-loop plant. The natural circulation analysis evaluated the effect of the HPVVs on natural circulation in a lowered-loop plant.

In the raised-loop analysis, the primary system was refilled with high pressure injection (HPI) as noncondensable gas was vented out the HPVVs and pressurizer PORV. Simulations were performed with and without the reactor vessel head vent line (RVHVL). The pressurizer PORV maintained the primary system pressure below the HPI shutoff head. In both simulations, the HPVVs adequately vented the noncondensable gases from the primary system. Ninety percent of the noncondensable mass was removed in the case with the vent line, while 85% was removed

without the vent line. The hot leg U-bends were refilled in both simulations.

The vent line analysis indicates that the bulk of the noncondensable gases in the upper head can be vented. There was, however, a 520-s delay in the time of the Loop B refill relative to the case without the vent line. Additionally, the analysis indicated that the vent line should be connected to the loop with the pressurizer because this loop fills faster than the other loop. This design will shorten the delay in loop refill, but the amount has not been determined.

Both raised-loop simulations demonstrated that if HPI is operated at its maximum rate, the net gravity head will not be adequate to sustain natural circulation after loop refilling. If HPI is isolated after the loops are refilled, core decay energy will eventually heat up the primary system and thereby establish density gradients sufficient to drive loop natural circulation. Additional analysis is required to develop operating strategies for throttling HPI to ensure recovery of natural circulation in a timely manner.

The HPI flow rate was not regulated to maintain the downcomer temperature within designated limits. This operator guideline was not modeled, because the purpose of this task was to investigate the effect of the RVHVL on primary system refill behavior. System refill times would be increased if HPI was throttled to maintain recommended subcooling in the downcomer region. Throttling HPI prior to refilling the loops would also help ensure a sufficient density gradient to maintain natural circulation after system refill. Additional analyses are required to quantify the operational strategies needed to ensure adequate core cooling while remaining within recommended pressure/temperature limits.

Noncondensable gas removal using only the HPVVs was estimated in the lowered-loop natural circulation analysis. The HPVVs removed 20% of the original noncondensable gas inventory in 2400 s. The noncondensable removal rate over the last 1300 s indicates that 59% of the noncondensable gas could be removed in 6900 s.

RELAP5/MOD2 calculated brief periods of loop stagnation. Operator and control system actions were not required to recover natural circulation. The maximum rates of noncondensable gas removal occurred during the loop stagnation periods, when the flow through the HPVVs was single-phase vapor.

The pressurizer heaters were unable to maintain the desired rate of primary system depressurization during

the periods of single-phase liquid HPVV flow. The heaters were effective at maintaining the desired rate of pressure decrease when the U-bends were two-phase, but were not able to recover the primary system pressure to the desired setpoint.

The HPI system recovered the primary system pressure in approximately 200 s after the primary system pressure was approximately 11 MPa

(1600 psia). After pressure recovery, the pressurizer PORV and the pressurizer heaters maintained the desired primary system pressure. The HPI system can recover primary system pressure, but the rate of non-condensable bubble expansion into the reactor vessel outlet plenum will be decreased.

The RELAP5/MOD2 analyses may be used to assist the NRC in evaluating noncondensable gas removal test data.

ACKNOWLEDGMENTS

The authors wish to acknowledge C. B. Davis for his review and technical assistance in the preparation of this report. Additionally, we wish to express our appreciation to E. E. Jenkins for the preparation of the report figures. Finally, we wish to acknowledge Walt Jensen, of NRC Nuclear Reactor Regulation (NRR), for his technical assistance in the development of the model, the conduct of the analyses, and his insightful comments in the review of the initial draft.

CONTENTS

ABSTRACT	ii
SUMMARY	iii
ACKNOWLEDGMENTS	v
INTRODUCTION	1
BACKGROUND INFORMATION	2
DESCRIPTION OF THE RELAP5/MOD2 MODELS	3
Primary System	3
Secondary System	8
Control Systems	8
Primary System Pressure Control	8
Secondary System Pressure Control	8
Steam Generator Level Control	8
Initial and Boundary Conditions	11
DISCUSSION OF ANALYSES	13
Results of Raised-Loop Analysis	13
Results of Lowered-Loop Analysis	19
CONCLUSIONS	27
Raised-Loop Primary System Refill	27
Lowered-Loop Noncondensable Gas Removal	27
REFERENCES	29

FIGURES

1. RELAP5/MOD2 nodalization of Loop A	4
2. RELAP5/MOD2 nodalization of Loop B	5
3. RELAP5/MOD2 nodalization of the pressurizer	6
4. RELAP5/MOD2 nodalization of the reactor vessel	7
5. RELAP5/MOD2 nodalization of the Loop A steam generator	9
6. RELAP5/MOD2 nodalization of the Loop B steam generator	10

7. Noncondensable mass inventories for the WRVHVL and WORVHVL cases	14
8. Reactor vessel upper head liquid levels for the WRVHVL and WORVHVL cases	14
9. Loop A and B mass inventories for the WRVHVL and WORVHVL cases	15
10. Mass flow rates into the down side of the Loop B U-bend for the WRVHVL and WORVHVL cases	17
11. Fluid temperatures at the top of downcomer and core outlet and saturation temperature for the WRVHVL case	18
12. Fluid temperatures at the top of downcomer and core outlet and saturation temperature for the WORVHVL case	18
13. System pressures for the WRVHVL and WORVHVL cases	19
14. HPVV mass flow rates for the WRVHVL and WORVHVL cases	20
15. Lowered-loop HPVV mass flow rates	20
16. Lowered-loop hot leg U-bend void fractions	21
17. Noncondensable mass at the lowered-loop vessel outlet	22
18. Lowered-loop hot leg U-bend mass flow rates	22
19. Desired and calculated lowered-loop primary system pressures	23
20. Lowered-loop primary system saturation temperature and hot leg liquid temperatures	24
21. Lowered-loop pressurizer PORV mass flow rate	24
22. Fraction of initial noncondensable gas removed from the lowered-loop primary system	25
23. Noncondensable mass in the lowered-loop vessel upper plenum	26
24. Lowered-loop fuel rod cladding surface temperatures at six axial elevations	26

TABLES

1. Initial and boundary conditions for the raised-loop calculations	11
2. Initial and boundary conditions for the lowered-loop calculations	12
3. Summary of raised-loop refilling times	13

VENTING OF NONCONDENSIBLE GAS FROM THE UPPER HEAD OF A B&W REACTOR VESSEL USING HOT LEG U-BEND VENT VALVES

INTRODUCTION

The Nuclear Regulatory Commission (NRC) requires that Babcock & Wilcox (B&W) plant licensees install remotely operated vents on the reactor vessel head for the removal of noncondensable gases.¹ Noncondensable gases in the primary system following a severe core damage accident might delay or retard natural circulation and inhibit core cooling during natural circulation.

Three B&W plants (Davis-Besse, Rancho Seco, and Crystal River) have temporary exemptions to the reactor vessel upper head vent requirement. These licensees contend that gases in the reactor vessel head can be discharged through the high point vent valves (HPVVs) without losing natural circulation or substantially delaying the time required to achieve natural circulation conditions.

This report provides confirmatory data regarding the licensees' proposals. The results may be utilized in the NRC staff review of requests for a permanent exemption to the head vent requirement.

Thermal-hydraulic analyses were performed using the RELAP5/MOD2² advanced reactor transient analysis computer code. An existing RELAP5/MOD2 model of a lowered-loop plant was used to develop a raised-loop model of a B&W plant. Hot leg U-bend

vent valves were added to both plant models. A vent line connecting the reactor vessel upper head to the Loop B steam generator inlet plenum was added to the raised-loop model.

Two simulations were performed using the raised-loop model, one with and one without a vent line connecting the reactor vessel upper head to the Loop B steam generator inlet plenum. Both analyses investigated plant refill behavior with the vessel initially filled to the vessel nozzles. The times required to refill the primary coolant system were evaluated.

Noncondensable gas removal using the hot leg U-bend vent valves was evaluated with the lowered-loop model. With the exception of the reactor vessel upper head, the primary system was liquid full. The vessel upper head was filled with a noncondensable gas (H₂), and natural circulation existed prior to the start of the calculation.

The following sections provide (a) background information regarding the installation of reactor vessel upper head vent valves, (b) a description of the RELAP5/MOD2 models used in the three calculations and summaries of the initial and boundary conditions, (c) relevant parameter responses, and (d) summaries of the conclusions derived from the analyses.

BACKGROUND INFORMATION

This section presents background information regarding the NRC requirement for the installation of a remotely operated vent on the reactor vessel head for noncondensable gas removal. The system is designed to vent noncondensable gas from the reactor coolant system which might inhibit core cooling during natural circulation.

During recovery following a severe core damage transient, the primary system is depressurized at a controlled rate. Noncondensable gases in the upper head will expand into the reactor vessel outlet plenum during the depressurization. A significant inventory of these gases in the coolant loops could stop natural circulation and subsequently decrease the plant heat removal rate. A reactor vessel upper head vent could remove these gases prior to the depressurization phase, thereby ensuring natural circulation conditions.

Three B&W plants (Davis-Besse, Rancho Seco, and Crystal River) have been issued temporary exemptions to the above head vent requirement. The licensees for these plants conclude that noncondensable gas in the reactor vessel will not affect core cooling and that the gas could be relieved through the vents in the reactor

system hot legs to the containment without loss of natural circulation.

The licensee for Davis-Besse proposes to vent the reactor vessel head to the inlet plenum of one steam generator instead of directly to the containment. This design provides for continuous flow of coolant through the reactor vessel head and would retard steam formation in the reactor vessel head during natural circulation cooldown. Nevertheless, for the case of noncondensable gas in the reactor vessel head, the flow of gas to a steam generator might retard decay heat removal in the steam generator. The flow of gas to the steam generator and HPVV might also delay the recovery of natural circulation conditions while the reactor coolant system is being refilled.

Thermal-hydraulic analyses evaluated primary coolant system refill while venting through the HPVVs and the PORV, and noncondensable gas removal using HPVVs. An Oconee-1 RELAP5/MOD2 model was modified to represent a raised-loop plant. The RELAP5/MOD2 code was modified to incorporate the physical properties of hydrogen. The analyses may be used to assist the NRC in evaluating test data that will be available in 1986.

DESCRIPTION OF THE RELAP5/MOD2 MODELS

This section presents a description of the RELAP5/MOD2 models. An existing RELAP5/MOD2 model of Oconee-1 was used, because the plant is similar to the Rancho Seco, Crystal River, and Davis-Besse plants. The Idaho National Engineering Laboratory (INEL) developed and quality assured the Oconee-1 model for the NRC Pressurized Thermal Shock Unresolved Safety Issue (USI-A49) program.³ The Oconee-1 model was modified to incorporate the HPVVs at the top of the hot leg U-bends. Further modifications were added to represent a raised-loop configuration. Additionally, control system actions that specifically addressed selected transient recovery procedures were added.

The RELAP5/MOD2 Oconee-1 model described major flow paths in the primary and secondary systems. The main feedwater system was not modeled, because the auxiliary feedwater sources were used in these analyses. The following sections describe the RELAP5/MOD2 models.

The raised-loop model was used to estimate primary system refill rates. One analysis included the reactor vessel head vent line (RVHVL) connecting the reactor vessel upper head to the inlet of the Loop B steam generator (WRVHVL). The other analysis was performed without the vent line (WORVHVL). Differences between the two calculations were analyzed to determine the effect of the RVHVL on system refill behavior. The vent line connected the vessel head to the loop without the pressurizer. The proposed design connects the vessel head to the loop with the pressurizer. The refill rate determined by the WRVHVL analysis is therefore conservatively longer than would occur with the proposed design.

The raised-loop plant differs from the lowered loop plant in the relative elevations of the major system components. The steam generators and pressurizer in the raised-loop plant are at a higher elevation relative to the reactor vessel. The vertical section of the hot legs is consequently longer, while the length of the cold leg suction piping is shorter and horizontal. The HPI system in the raised-loop model was low-head, while the lowered-loop model simulated a high-head system. Low pressure injection was not simulated in either model.

The lowered-loop model was used to evaluate non-condensable gas removal from the reactor vessel head using the HPVVs. The modeled plant was in the natural circulation cooldown phase following a severe core damage accident.

A RELAP5/MOD2 error in extrapolating water properties from the upstream volume to the HPVV became apparent during this task. The HPVV flows were higher than HEM flows for the same thermodynamic conditions. The problem occurred in the critical flow model when upstream break conditions were characterized by low void fractions ($1.0E-5$ or less) with a noncondensable present. The problem was addressed by introducing an intermediate volume between the U-bend and the boundary volume. The frictionless horizontal volume flow area was the same as the HPVV flow area.

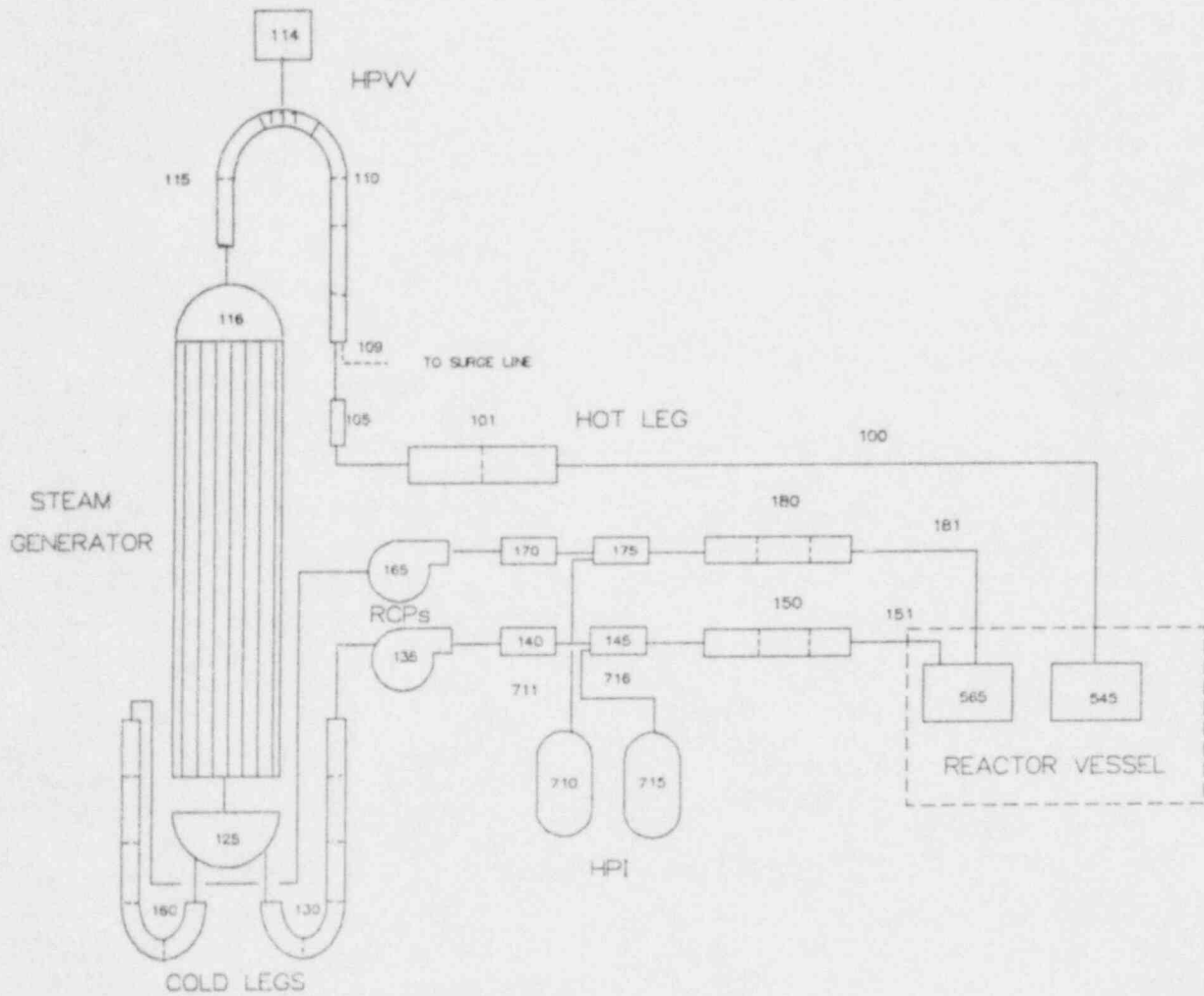
Primary System

Figures 1 and 2 show the primary loop configurations. The B&W plants are a 2-by-4 configuration. Each consists of one hot leg, two cold legs, and a steam generator. Each cold leg consists of a pump suction leg, a coolant pump, and a pump discharge leg. The lowered-loop plants have a cold leg loop seal, while the raised-loop plant does not. Additionally, because the raised-loop steam generators are higher relative to the reactor vessel, the hot leg vertical sections are longer.

Figure 3 shows the surge line and pressurizer. The surge line connected the pressurizer to the Loop A hot leg. The pressurizer PORV was attached to the upper head of the pressurizer. The pressurizer safety valves were not included in the model. Pressurizer heaters and associated controls were also modeled. The pressurizer spray lines were not modeled, because the reactor coolant pumps were tripped, thereby eliminating sufficient driving head to overcome the large elevation difference between the cold leg and the top of the pressurizer.

Figure 4 shows the RELAP5/MOD2 reactor vessel model. The model describes the inlet annulus, downcomer, lower plenum, core, core bypass, upper plenum, upper head, and reactor vessel internal vent valves. The vent line connected component 550-02 to component 216-01 in the raised-loop model. The vent line was not simulated in the lowered-loop model.

All components were modeled with the RELAP5/MOD2 nonequilibrium and nonhomogeneous models. Wall friction, choking, and horizontal and vertical stratification were also applied in every component. The choking model, two-velocity model, and smooth area change model were applied at all junctions. Junctions were centrally connected with the exception of the hot leg HPVV junctions. The HPVVs were



EEJ00208

Figure 1. RELAP5/MOD2 nodalization of Loop A.

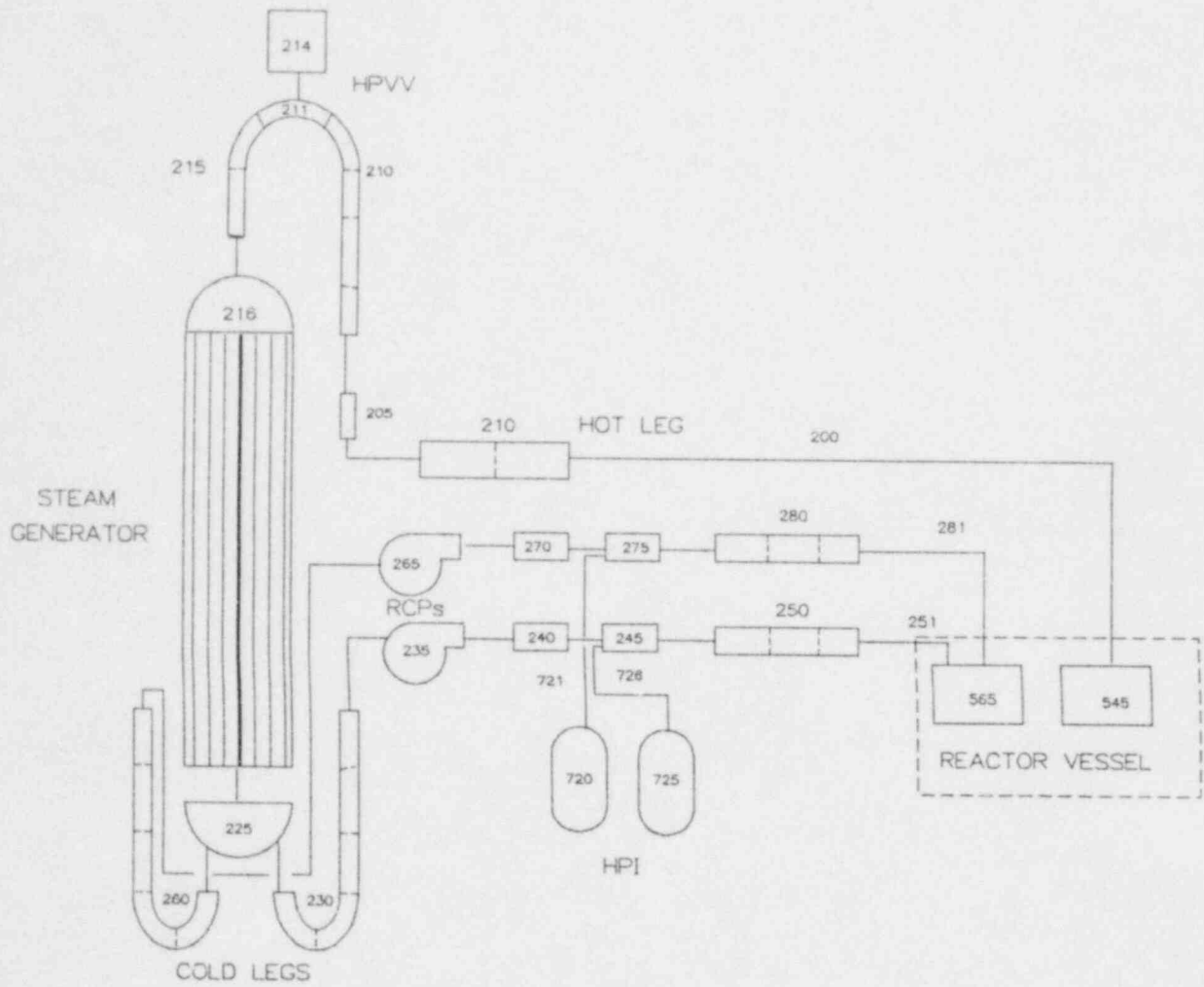


Figure 2. RELAP5/MOD2 nodalization of Loop B.

EEJ00211

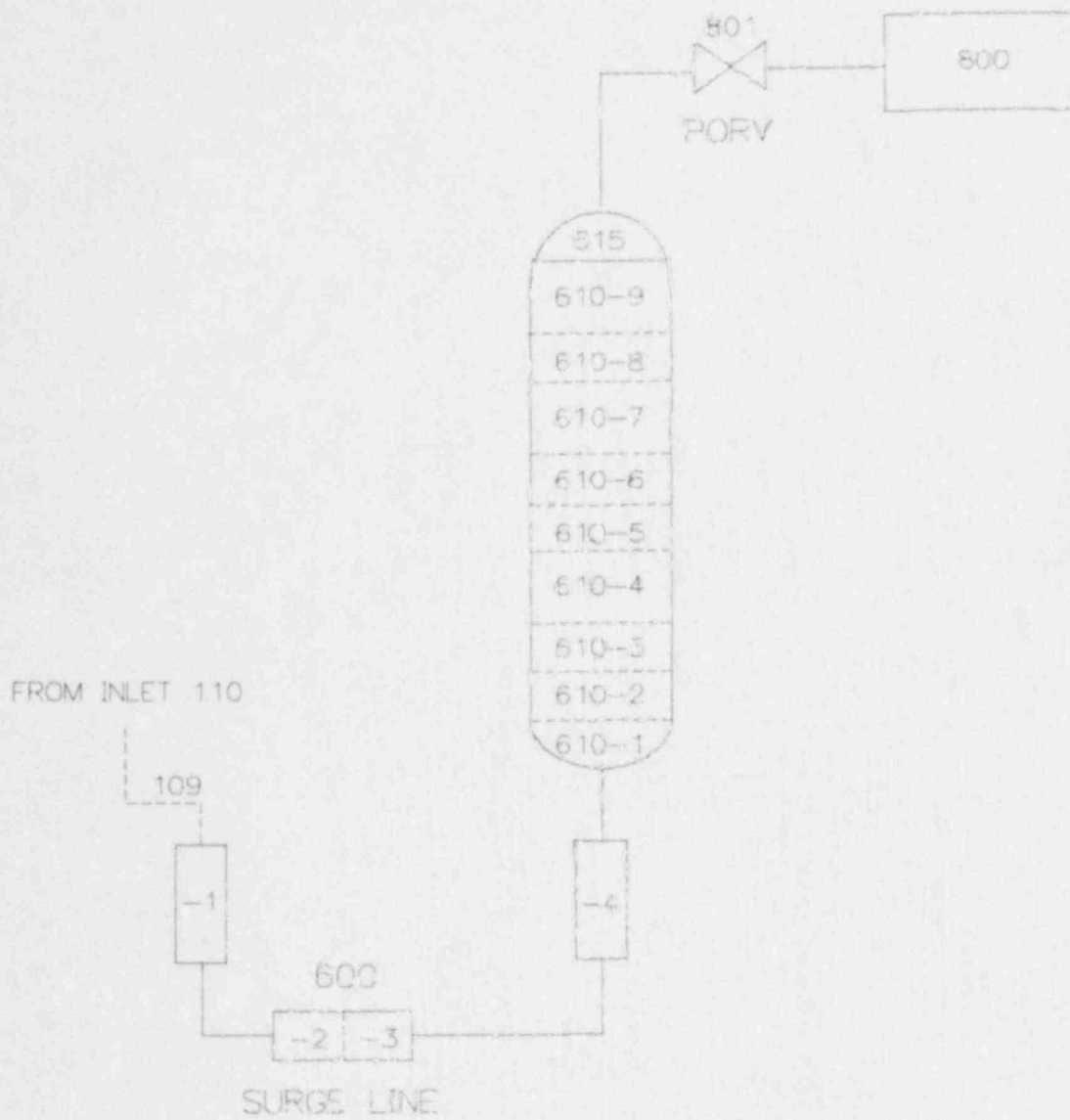


Figure 3. RELAP5/MOD2 nodalization of the pressurizer.

EEJ002/12

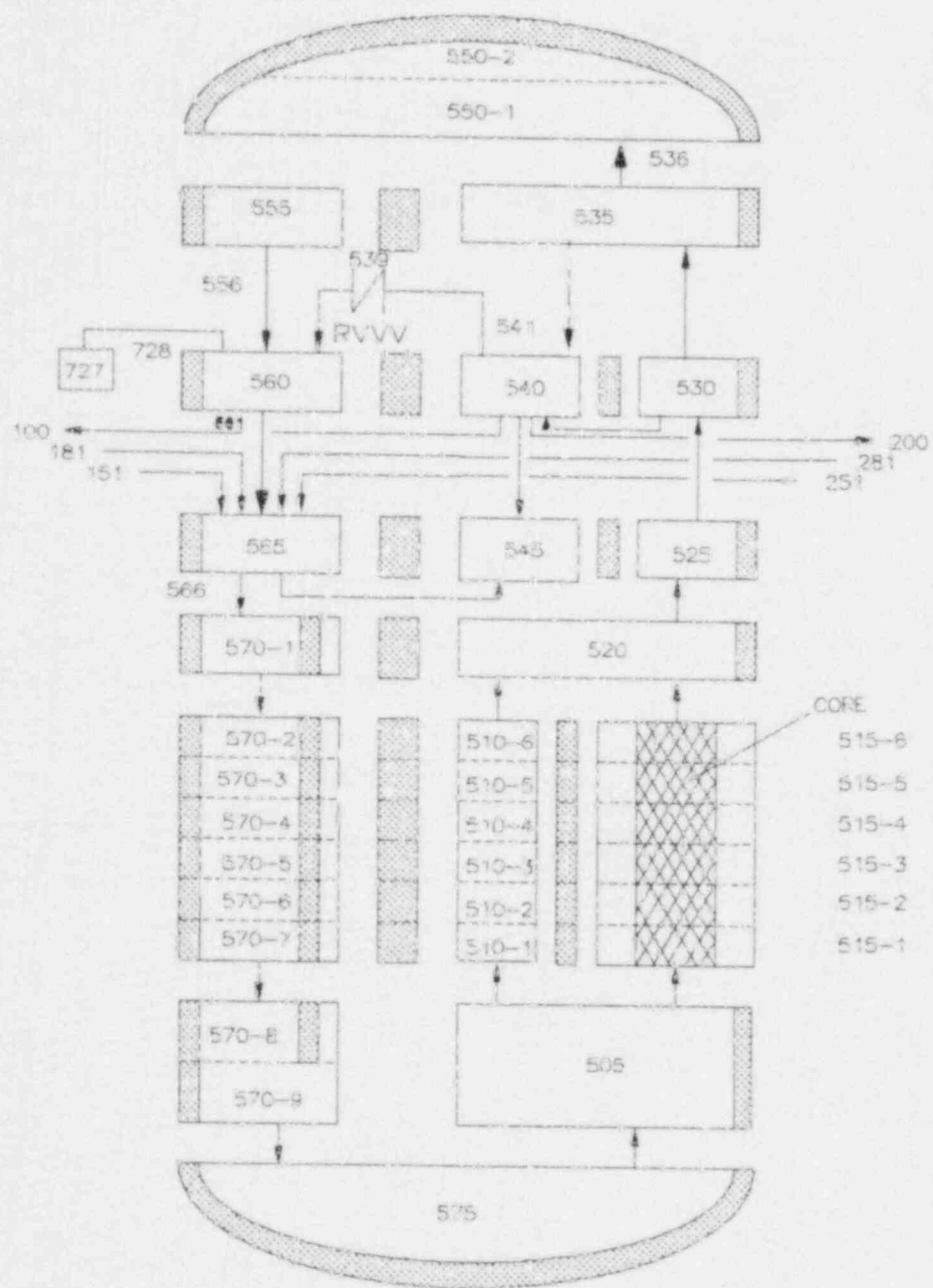


Figure 4. RELAP5/MOD2 nodalization of the reactor vessel.

EEJ00213

connected to the tops of the hot legs to represent the actual plant configuration.

Heat structures representing the fuel rods, steam generator tube bundles, pressurizer heaters, and the piping and component walls were included in both models.

Secondary System

Figures 5 and 6 show the RELAP5/MOD2 models of the A and B steam generator secondary systems. Only the emergency feedwater sources and headers were modeled for the feedwater sources. The main feedwater system is normally valved out during the period of transient recovery studied in this investigation.

The steam generator models consisted of the following:

- An annular downcomer,
- An adjustable orifice plate at the bottom of the downcomer,
- The heat exchange region,
- The aspirator ports between the heat exchange region and the downcomer,
- The steam outlet annulus,
- A junction connecting the emergency feedwater header to the top of the heat exchange region,
- The main steam lines, and
- A turbine bypass valve.

The main steam lines were modeled using three volumes to represent each steam line. A single valve on each line represented the turbine bypass valve. This analysis did not require either the safety relief valves or the turbine governor/stop valves.

Control Systems

Control systems were modeled to regulate primary system pressure, heat removal, inventory, and steam generator levels. This section briefly describes these control systems.

Primary System Pressure Control

In the raised-loop calculations, the primary system was initially depressurized to 6.9 MPa (1000 psia) using the pressurizer PORV. The PORV then maintained the primary system near this pressure.

HPI operated continuously at its maximum flow rate in the raised-loop calculations to simulate primary

system refill. HPI throttling was not modeled, although typical operator procedures include requirements to maintain the primary system pressure and temperature within recommended limits. This was done so that operator procedures would not mask comparisons between the two raised-loop calculations. The total HPI capacity was 0.031 m³/s (1.1 ft³/s) at a backpressure of 0.17 MPa (25 psi).

In the lowered-loop calculation, the primary system pressure was to be reduced at a constant rate of 0.002 MPa/s (0.32 psi/s) using the pressurizer PORV and heaters. The PORV opened when the pressure in the pressurizer exceeded the desired pressure and the subcooling in the hot legs was more than 55.6 K (100°F). The PORV remained open until the subcooling in the hot legs decreased to 14 K (25°F) or the pressure decreased below the desired value. The PORV open/close time was 2 s.

The pressurizer heaters assisted in pressure recovery when the hot leg temperature became less than 14 K (25°F) subcooled or when the primary system pressure was below the desired value. The heaters remained on until the subcooling in the hot legs reached 55.6 K (100°F). The heaters were turned off if the pressurizer level decreased below 2.6 m (8.7 ft). The total heater capacity was 1.68 MW.

In the lowered-loop calculation, HPI assisted in recovery of subcooling in the hot and cold legs and in recovery of pressurizer level. HPI was initiated when the minimum subcooling in either loop was less than 27.8 K (50°F) or the pressurizer level was less than 50%. The HPI remained on until the minimum subcooling reached 55.6 K (100°F) and the level exceeded 50%. As in the raised-loop calculations, HPI flow was not throttled. The total HPI capacity was 0.068 m³/s (2.4 ft³/s) for atmospheric conditions.

Secondary System Pressure Control

The turbine bypass valves depressurized the secondary system pressure to 1.05 MPa (150 psia) at the start of the raised-loop calculations. The rapid depressurization simulated operator actions performed to increase the potential for natural circulation.

The turbine bypass valves depressurized the secondary system 0.001 MPa/s (0.16 psi/s) in the lowered-loop calculation. This corresponded to approximately 0.015 K/s (0.028 °F/s). A linear depressurization rate was used, because the error in the rate of temperature decrease was insignificant for this analysis.

Steam Generator Level Control

Steam generator levels were maintained at 95%

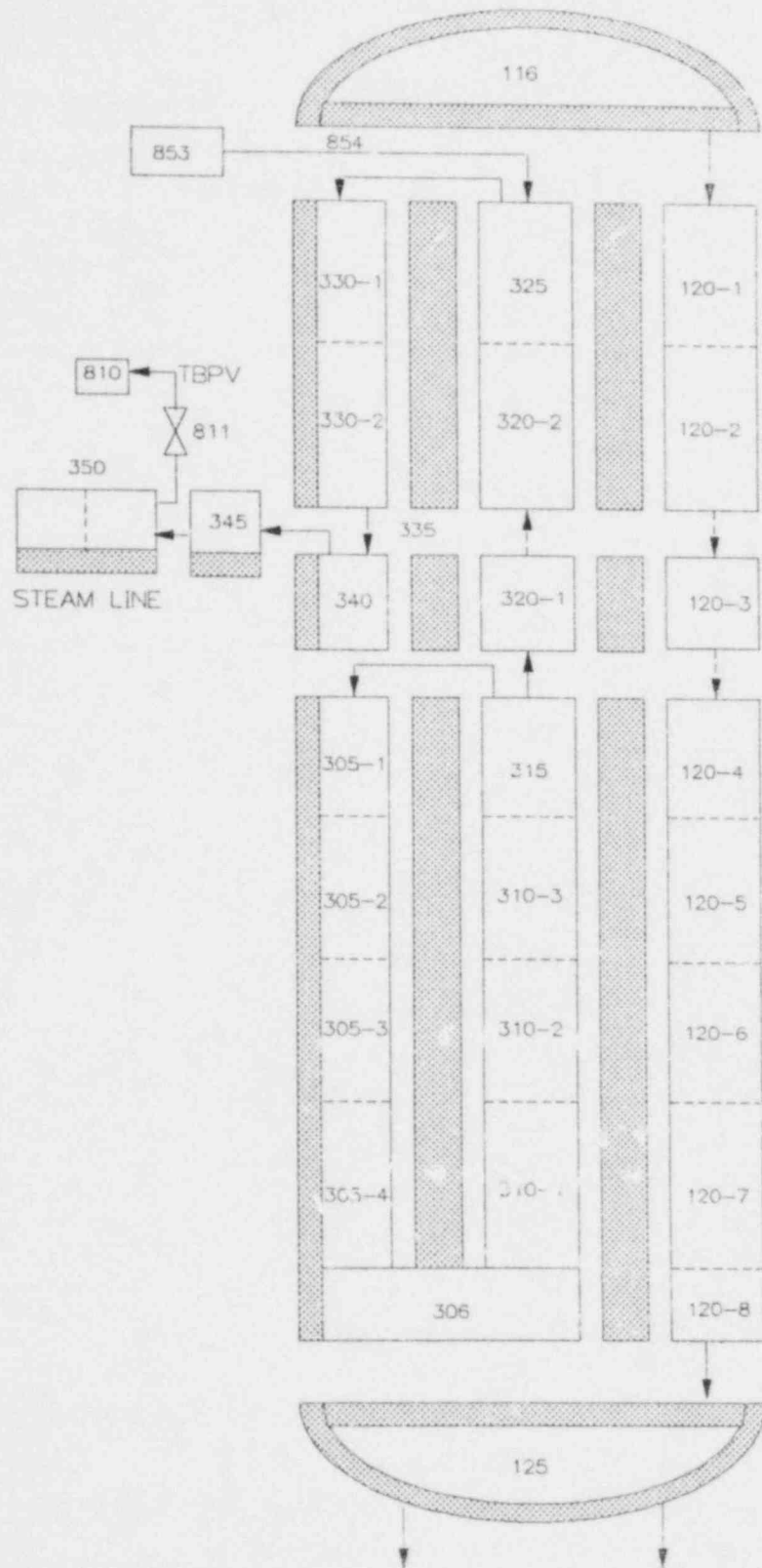


Figure 5. RELAP5/MOD2 nodalization of the Loop A steam generator.

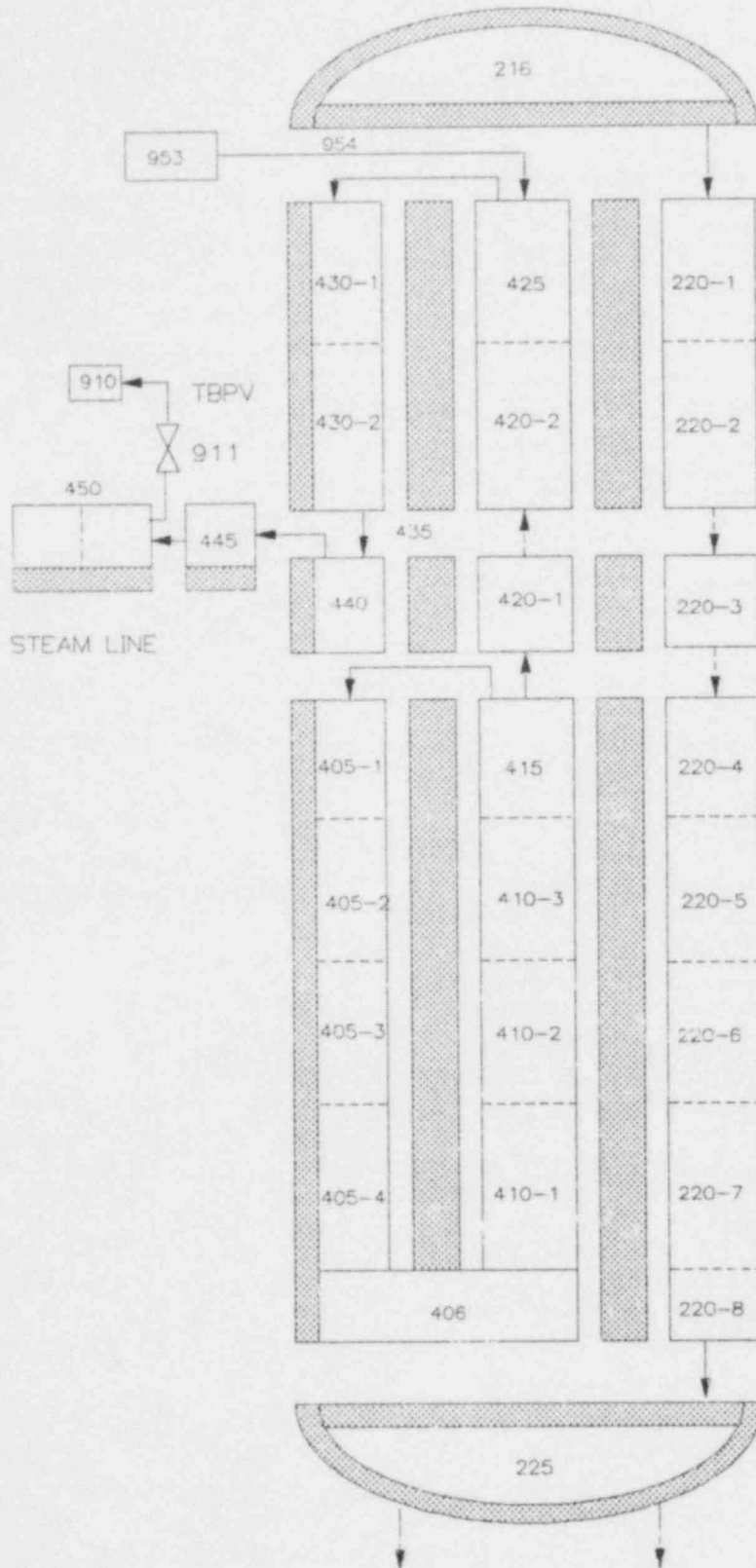


Figure 6. RELAP5/MOD2 nodalization of the Loop B steam generator.

operating level with the emergency feedwater (EFW) system. EFW started when the level in the corresponding steam generator decreased 0.127 m (0.417 ft) below the setpoint. The EFW remained on until the steam generator level increased to 0.127 m (0.417 ft) above the setpoint.

In the lowered-loop calculation, the turbine bypass valves closed in 4 s when the steam generator level decreased below 6.9 m (22.7 ft). The steam generator level had priority over the setpoint pressure to ensure natural circulation in the primary coolant loops.

Initial and Boundary Conditions

Table 1 summarizes the initial and boundary conditions used in the raised-loop calculations. The calculations were initiated from conditions representing a severe core damage accident after the vessel had been refilled to the vessel nozzles. The core power represented ANS decay power 2 h after a reactor scram. Approximately half of the primary system was occupied by a hydrogen-steam mixture. Hydrogen concentrations were located in the vessel upper head, upper plenum, and the vertically oriented regions of the primary coolant piping. The pressurizer level was reduced to 30% at the start of the calculations. Stagnant conditions existed in both coolant loops. HPI was

not being injected, because the primary system pressure was greater than the HPI shutoff head.

Table 2 summarizes the initial and boundary conditions used in the lowered-loop calculation. The initial and boundary conditions in the lowered-loop calculation represented a recovered plant 2 h after a severe core damage accident. With the exception of the reactor vessel upper head, the primary system was liquid full. The reactor vessel upper head contained approximately 95% hydrogen (by volume). The reactor coolant pumps were assumed to be damaged and out of service. Natural circulation conditions existed in both coolant loops. The steam generator secondary operating levels were maintained at 95%. Natural circulation of the primary system fluid through the steam generators removed the reactor decay heat.

The steam generator outlet plenum temperature was higher than the inlet temperature at the start of the calculation. The modeling of EFW injection to maintain level caused the heat transfer from the primary system to the secondary system to slowly oscillate between positive and negative values. This did not affect the results of the analysis, because events during the calculation overwhelmed EFW injection effects. The energy transferred to the steam generator secondary heated the subcooled EFW (at 306 K, 91 °F) to near saturation conditions. Hence, the steam generation rate was insignificant.

Table 1. Initial and boundary conditions for the raised-loop calculations

Parameter	Value	
Primary system		
Power, MW	30.0	
Hot leg temperature, K (°F)	544.0	(520.0)
Cold leg temperature, K (°F)	544.0	(520.0)
Pressure, MPa (psia)	11.34	(1645.0)
Mass flow rate, kg/s (lbm/s)	0.0	(0.0)
Volume of hydrogen, m ³ (ft ³)	158.6	(5600.0)
Mass of hydrogen, kg (lbm)	390.0	(860.0)
Secondary system		
Pressure, MPa (psia)	6.68	(969.0)
Temperature, K (°F)	555.0	(540.0)
SG collapsed level, m (in.)	3.05	(120.0)
EFW mass flow rate, kg/s (lbm/s)	0.0	(0.0)
EFW temperature, K (°F)	306.0	(91.0)

Table 2. Initial and boundary conditions for the lowered-loop calculations

Parameter	Value	
Primary system		
Power, MW	28.3	
Hot leg temperature, K (°F)	554.0	(537.6)
Cold leg temperature, K (°F)	555.9	(541.0)
Pressure, MPa (psia)	16.8	(2432.8)
Mass flow rate, kg/s (lbm/s)	239.5	(528.0) Loop A
	222.3	(490.0) Loop B
Volume of hydrogen, m ³ (ft ³)	13.4	(472.0)
Mass of hydrogen, kg (lbm)	87.4	(192.7)
Secondary system		
Pressure, MPa (psia)	6.5	(945.0)
Temperature, K (°F)	554.3	(538.0)
SG operating level, m (in.)	6.9	(272.0)
EFW mass flow rate, kg/s (lbm/s)	29.0	(65.0)
EFW temperature, K (°F)	305.9	(91.0)

DISCUSSION OF ANALYSES

The following sections describe the results of the raised-loop and lowered-loop analyses.

Results of Raised-Loop Analysis

The refill calculations were initiated by opening the pressurizer PORV. This depressurized the primary system to 6.9 MPa (1000 psia), thereby ensuring HPI flow for primary system refill. The PORV opened whenever the system pressure exceeded 6.9 MPa (1000 psia). The HPVVs were also opened at the start of the calculations, and the steam generator secondary systems were depressurized to 1.05 MPa (150 psia) by opening the turbine bypass valves. The HPI system operated at its maximum possible flow rate during the calculation. The reactor coolant and charging pumps were assumed to be inoperative.⁴

The refill analysis determined the effect of a RVHVL on the rate of primary system refill. Consequently, the HPI was not throttled to control the vessel downcomer fluid temperature within typical recommended pressure/temperature limits.

The analysis indicates it is possible to refill the primary system using HPI to the point where natural circulation can be established. The analysis also indicates it is possible to vent the bulk of the hydrogen trapped in the primary system through the HPVVs. Table 3 summarizes the refill times for each calculation. The Loop B U-bend was filled on both sides (bridged) 520 s earlier in the WORVHVL case than in the WRVHVL case. The bridging of the Loop B U-bend signified the final stage of primary system

refilling in each calculation. Bridging of the loop U-bends is a necessary condition for establishing natural circulation.

The calculated noncondensable mass inventory responses are shown in Figure 7 for the WRVHVL and WORVHVL cases. Approximately 85 and 90% of the noncondensable inventory was removed by the HPVVs in the WORVHVL and WRVHVL calculations, respectively. The noncondensable removal rates were similar during the first 3000 s of the calculations. Noncondensable gas trapped in the reactor vessel upper head in the WORVHVL calculation caused the difference in responses after 3000 s.

The pressurizer PORV was open for substantial periods in both calculations and was the main pathway by which liquid escaped from the primary system. The pressurizer refilled during the first 400 s, which removed the noncondensable gas that was originally in the pressurizer. The noncondensable gas in the Loop A hot leg was above the elevation where the pressurizer surge line connected to the hot leg of Loop A. Consequently, the noncondensable gas in the loops and reactor vessel was removed from the primary system through the HPVVs.

Figure 8 compares the collapsed liquid levels in the vessel upper head. The vessel upper head began refilling at 650 and 1457 s in the WRVHVL and WORVHVL cases, respectively. In the WRVHVL case, a significant amount of the steam/hydrogen bubble was displaced from the upper head via the RVHVL to Loop B. A period of rapid vapor condensation in the WRVHVL calculation caused a relatively rapid

Table 3. Summary of raised-loop refilling times

Event	Time With RVHVL (s)	Time Without RVHVL (s)
Calculation initiated, PORV opened, HPVVs opened, HPI started	0	0
Loop A filled to U-bend, up side/down side	1920/2297	2210/2574
Loop B filled to U-bend, up side/down side	3235/3464	2398/2943
End of calculation	3900	3300

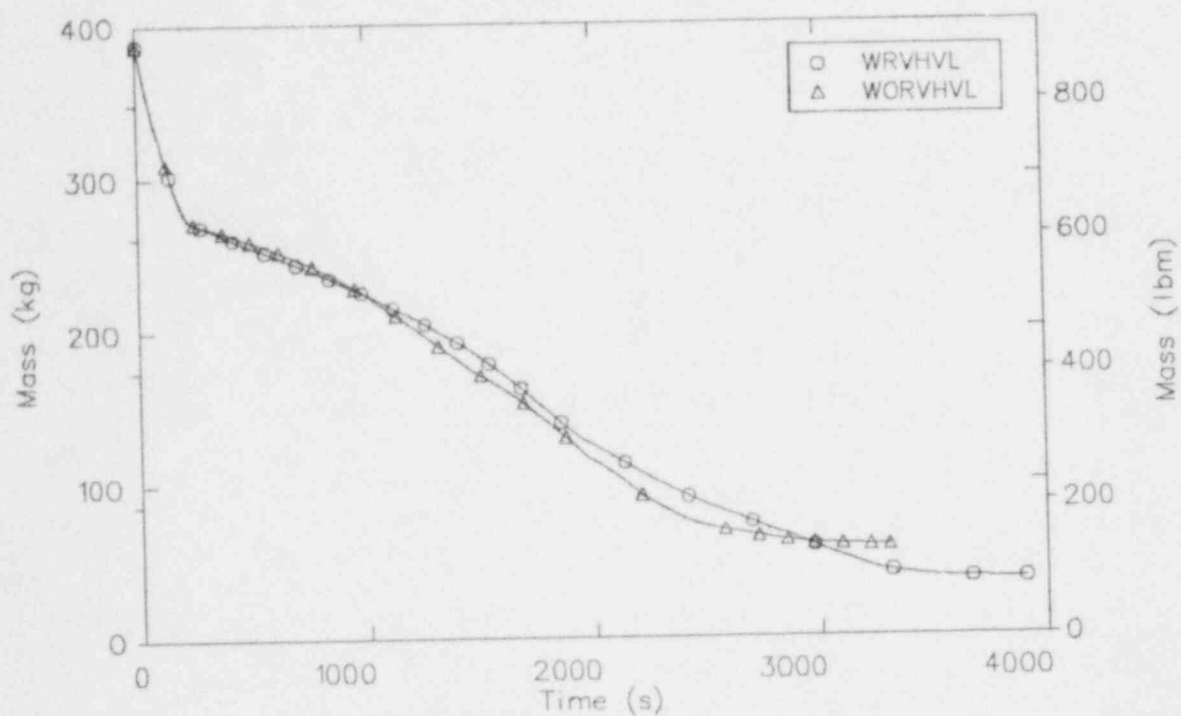


Figure 7. Noncondensable mass inventories for the WRVHVL and WORVHVL cases.

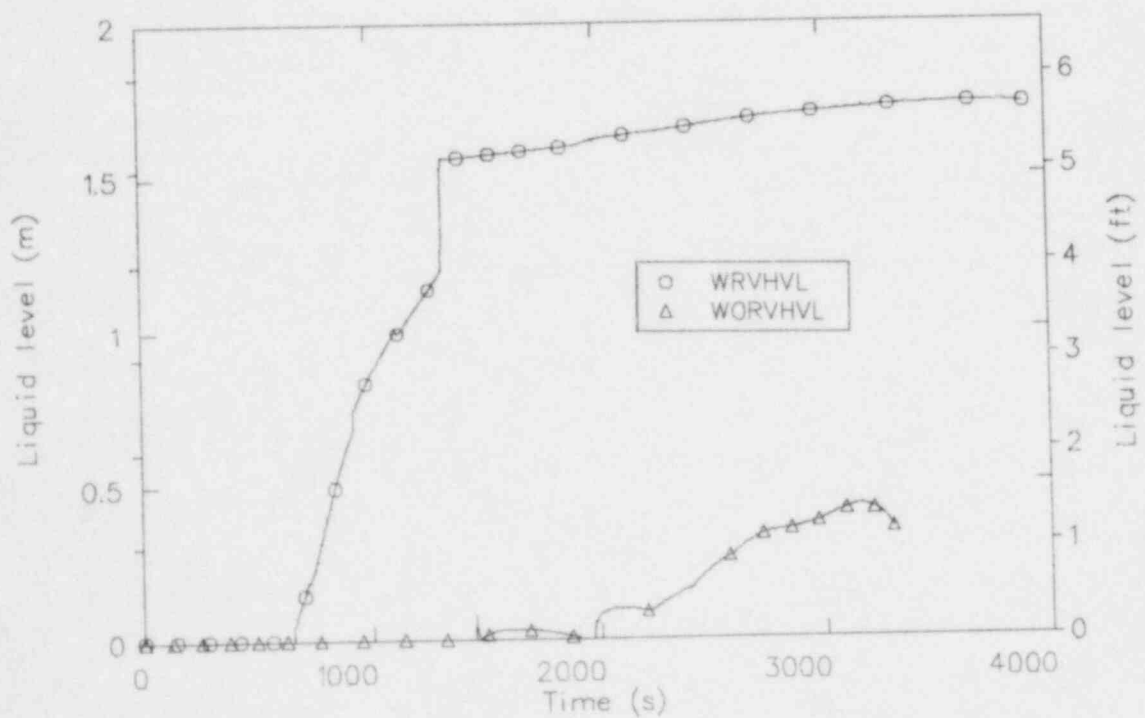


Figure 8. Reactor vessel upper head liquid levels for the WRVHVL and WORVHVL cases.

level increase from 1.2 m (3.94 ft) to 1.6 m (5.25 ft) between 1315 s and 1323 s. The vessel upper head was almost completely filled in the WRVHVL simulation. In contrast, in the WORVHVL simulation, the vessel upper head level was calculated to be less than 25% of full span.

In the WORVHVL simulation, the steam/hydrogen bubble was trapped in the reactor vessel head. As the primary system refilled, the upper head gas bubble was partially compressed, allowing some liquid to be displaced into this region. This produced a compressional reaction force that retarded further refill of the upper head region. Consequently, the path of least resistance from the vessel upper plenum region was into the loops.

Figure 9 compares the calculated loop mass responses for the WRVHVL and WORVHVL simulations. The total loop mass inventory initially decreased in both simulations due to the initial refill of the pressurizer. By 400 s, the loop mass inventories had either begun to increase (Loop A) or had temporarily stabilized before increasing (Loop B).

The initially larger Loop A mass was the consequence of the pressurizer being located on Loop A. In the course of calculating the initial conditions prior to the transient, the pressurizer PORV was employed to control system pressure as the hydrogen was injected

into vessel. The operation of the PORV resulted in more mass being distributed initially to Loop A.

In the WRVHVL simulation, the mass inventory in Loops A and B decreased for approximately 200 and 400 s, respectively. After 200 s, the Loop A mass inventory began to increase. At 400 s, when the pressurizer refilled, the Loop B mass inventory reached a minimum and began to significantly increase at approximately 1000 s. At 1000 s, the mass in Loop A (52,000 kg) was almost twice as large as the mass in Loop B (28,000 kg). Also by this time, the rapid displacement of gas from the vessel upper head via the RVHVL had ended and both Loops A and B began to refill at approximately the same rate. By 1920 s, the up side of the Loop A U-bend was refilled; and the loop mass remained nearly constant for the remainder of the transient. The refill response of Loop B was delayed but similar to Loop A after 1000 s. At 3235 s, the up side of the U-bend was filled; and the up side and down side of the U-bends were refilled at 3464 s.

The RVHVL in Loop B was the principal reason why the refill of Loop B was delayed relative to Loop A in the WRVHVL simulation. This was the consequence of the steam/hydrogen bubble in the WRVHVL simulation being displaced into Loop B as the primary system was refilled by HPI. The bubble in the vessel head was displaced to Loop B as a result

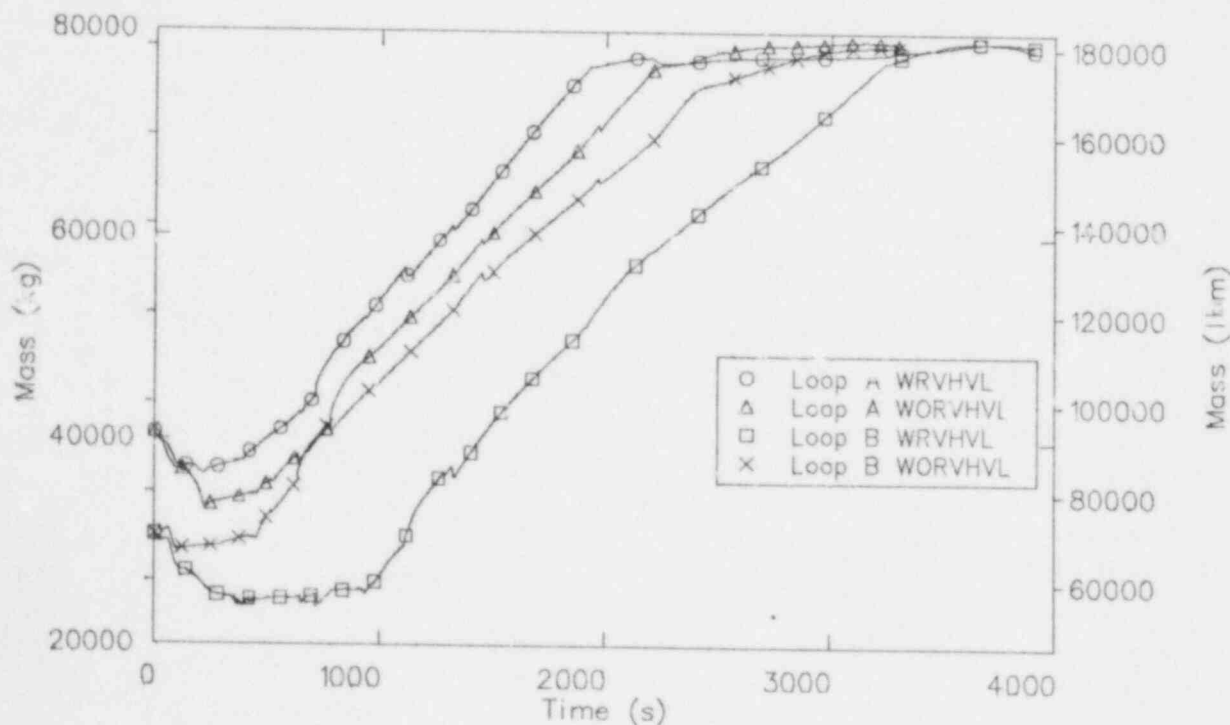


Figure 9. Loop A and B mass inventories for the WRVHVL and WORVHVL cases.

of a positive differential pressure between the top of the U-bend and vessel head. Buoyancy forces contributed to this differential pressure, since the U-bend/RVHVL interface is above the vessel head. HPI injection also contributed to this differential pressure, because the injection of liquid into the primary system tended to "squeeze" the lighter trapped gasses out of the system via the HPVV pathways.

In the WORVHVL simulation, the loop mass inventories initially decreased due to pressurizer filling. The Loop A mass inventory began to increase at 200 s and Loop B at 400 s. Relative to the mass initially lost from Loop B during the first 400 s. This was, in part, due to the higher liquid levels in Loop A versus Loop B in the steam generator and U-bend regions. In particular, during the first 200 s, the higher levels in Loop A caused liquid to be transferred to Loop B to establish loop-to-loop gravity head balance. By 900 s, both loops had approximately the same mass inventories. After this period, Loop A had 4000-6000 kg more mass than Loop B. The principal reason Loop A had a larger net mass was that the pressurizer was located on Loop A. Since the pressurizer PORV was open during most of the transient, there was a period of preferential flow to Loop A at the expense of Loop B. This mass difference was sufficient to cause a delay of about 370 s between the times the top of Loop A and Loop B were refilled (see Table 3). Hence, the presence of the pressurizer tends to delay loop refill of the other loop. A further discussion pertaining to the pressurizer location will be given later.

The most significant difference between the mass responses in the WRVHVL and WORVHVL calculations was that it took Loop B approximately 520 s longer to refill in the WRVHVL simulation. This was the consequence of the RVHVL. As previously explained, in the WRVHVL analyses the RVHVL tends to cause a delay in the refilling of Loop B but enhances the refilling of the vessel. On the other hand, the WORVHVL simulation demonstrated that without the RVHVL the loop refilling responses were more symmetric and Loop B refilled earlier. The earlier loop refilling was done at the expense of vessel refilling, since a steam/hydrogen bubble remained trapped in the vessel upper head in the WORVHVL simulation.

Venting the noncondensable gas from the vessel upper head to the loop without the pressurizer delayed the refill of Loop B. If the RVHVL had been connected to Loop A, the opened PORV could have mitigated the effect of the noncondensable bubble trapped in the steam generator inlet plenum. A preliminary analysis indicates that with the RVHVL connected to the loop

with the pressurizer, the refill behavior of the two loops was similar to the WORVHVL case. Additionally, since Loop A refilled 370 s faster than Loop B, it is recommended that the RVHVL be connected to the loop with the pressurizer. This conclusion is in agreement with the proposed Davis-Besse RVHVL design. The analysis in this report was performed with the vent line connected to the loop without the pressurizer. This model yielded the most conservative results with regard to the rate of primary system refill.

Figure 10 compares the calculated mass flow rates into the down side of the Loop B U-bend for the two calculations. The refilling of the U-bend up sides resulted in the onset of flows at 2398 and 3235 s in the WORVHVL and WRVHVL cases, respectively. The peak flow rates occurring at 2943 and 3464 s correspond to the times when Loop B was filled to the U-bend in the WORVHVL and WRVHVL calculations. Similar flow behavior occurred in Loop A coincident with refilling the up and down sides of the U-bends.

In both the WRVHVL and WORVHVL simulations, conditions did not promote loop natural circulation after U-bend bridging. Unthrottled HPI entering the reactor vessel decreased the average vessel fluid temperature below the average temperature in the vertical sections of the steam generator tube bundles. Moreover, the fluid temperature in the tube bundles was approximately the same as the temperature of the fluid in the steam generator secondaries. Consequently, significant primary-to-secondary heat transfer was not calculated after U-bend bridging. The resulting net density head between the vessel and loops was not sufficient to drive loop natural circulation. As a consequence, the only natural circulation path that existed was between the downcomer and core via the reactor vessel vent valves.

If HPI had been throttled to maintain a recommended downcomer fluid temperature, the density head generated by core decay heat would have been sufficient to drive loop natural circulation. Additionally, after U-bend bridging, the primary-to-secondary heat transfer would have maintained an adequate steam generator density gradient for natural circulation.

If HPI had been throttled after the loops were refilled, core decay energy would have eventually heated the primary system, thereby establishing adequate natural circulation gradients. If the HPI is throttled, it must be regulated so that liquid losses through the PORV do not cause voiding in the U-bends. It was estimated that natural circulation could be established 45 min after loop refill if HPI were throttled while the primary system pressure was maintained at 6.9 MPa (1000 psia).

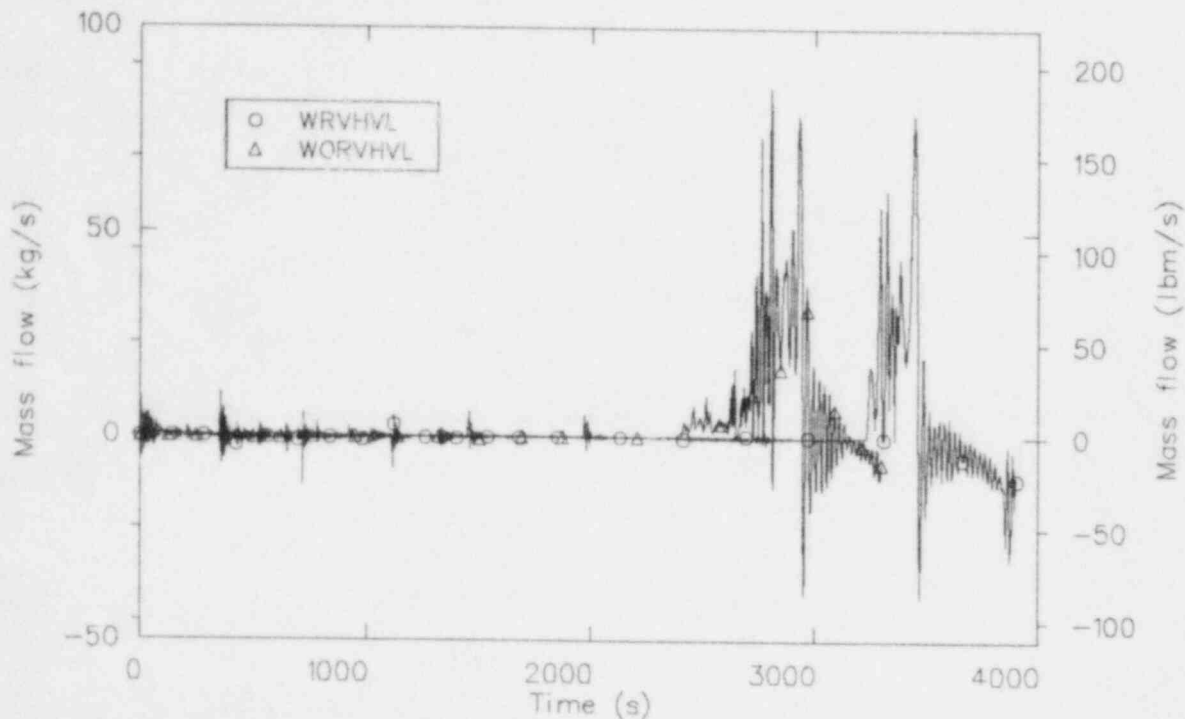


Figure 10. Mass flow rates into the down side of the Loop B U-bend for the WRVHVL and WORVHVL cases.

The reactor vessel vent valve located between the vessel upper plenum and the top of the downcomer provided a natural circulation path within the reactor vessel. This circulation maintained core cooling via mixing of HPI entering the downcomer and passing into the core region. The liquid in the reactor vessel remained subcooled throughout the calculations, and the cladding temperatures did not exceed those found during normal operating conditions.

Figures 11 and 12 are comparisons of the calculated fluid and saturation temperatures at the top of the downcomer and upper plenum for the WRVHVL and WORVHVL simulations. The maximum subcooling was calculated at 300 s and 400 s and equaled 200 K (360°F) and 220 K (400°F) at approximately 6.9 MPa (1000 psia) for the WRVHVL and WORVHVL simulations, respectively. The final subcooling for both simulations was approximately 178 K (320°F) at a pressure of 9.6 MPa (1390 psia). It is observed from Figures 11 and 12 that maximum subcooling occurred early in the simulations at a time prior to any significant flow through the vessel vent valves. Once the vent valves opened, the resultant downcomer/upper plenum mixing reduced subcooling in the downcomer and decreased the upper plenum temperature. Before mixing was initiated, the plenum temperature was only slightly subcooled.

The downcomer temperature was not regulated because these analyses were performed to determine the effect of a RVHVL on refilling the coolant loops. Consequently, the vessel downcomer fluid temperature was less than that found in typical pressure/temperature operating envelopes. Typically, at pressures from 6.9 to 9.7 MPa (1000 to 1410 psia), subcooling temperatures less than 27.8 K (50°F) are desired.⁴ For a particular HPI throttling strategy to be effective, the total HPI flow rate must exceed the PORV flow rate. Additional analysis is recommended to determine the appropriate operational strategies for HPI throttling following a severe core damage accident.

Presented in Figure 13 are the calculated pressure responses for the WRVHVL and WORVHVL simulations. Both pressure responses were characterized by an initial 200-s period of depressurization from 11.34 MPa (1645 psia) to 6.9 MPa (1000 psia) when the PORV was opened. During the periods of 200-1000 s and 200-2300 s, the calculated pressure responses for the WRVHVL and WORVHVL simulations were relatively constant at 6.9 MPa (1000 psia). Pressure increases occurred when certain steam/hydrogen regions in the primary system were compressed.

The principal regions that controlled the pressure increases were located in the vessel upper head and inlet annulus (Figure 4). In particular, the upper head

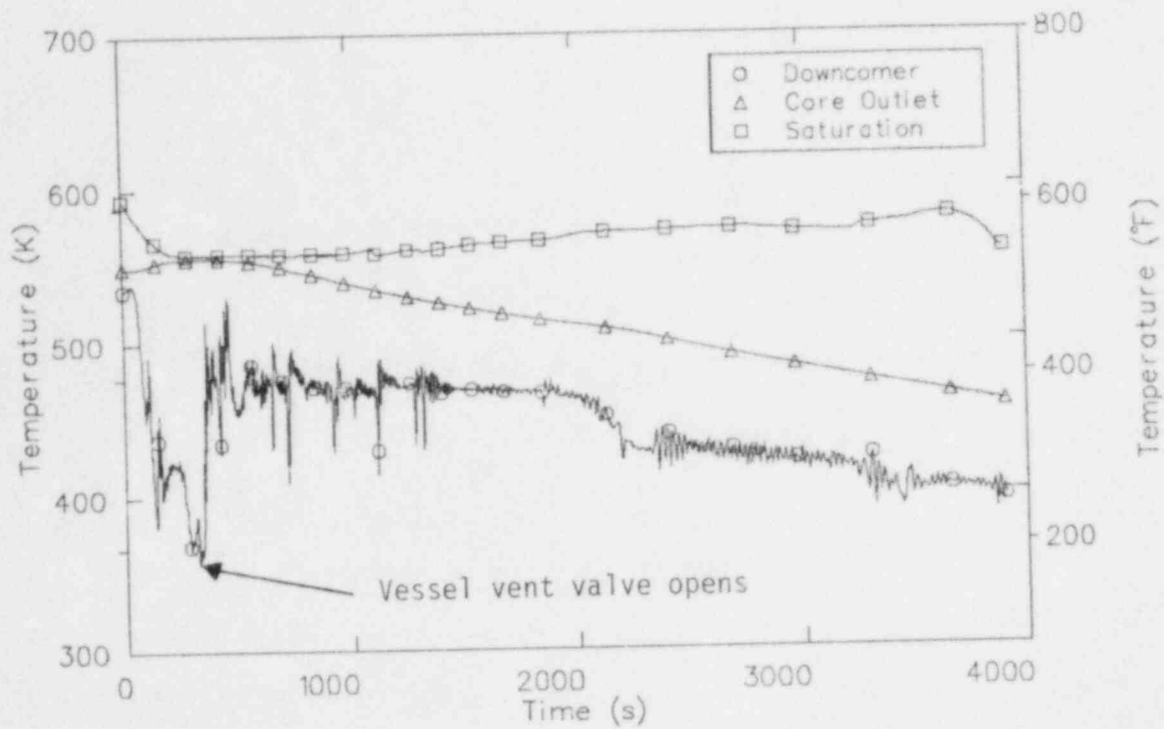


Figure 11. Fluid temperatures at the top of downcomer and core outlet and saturation temperature for the WRVHVL case.

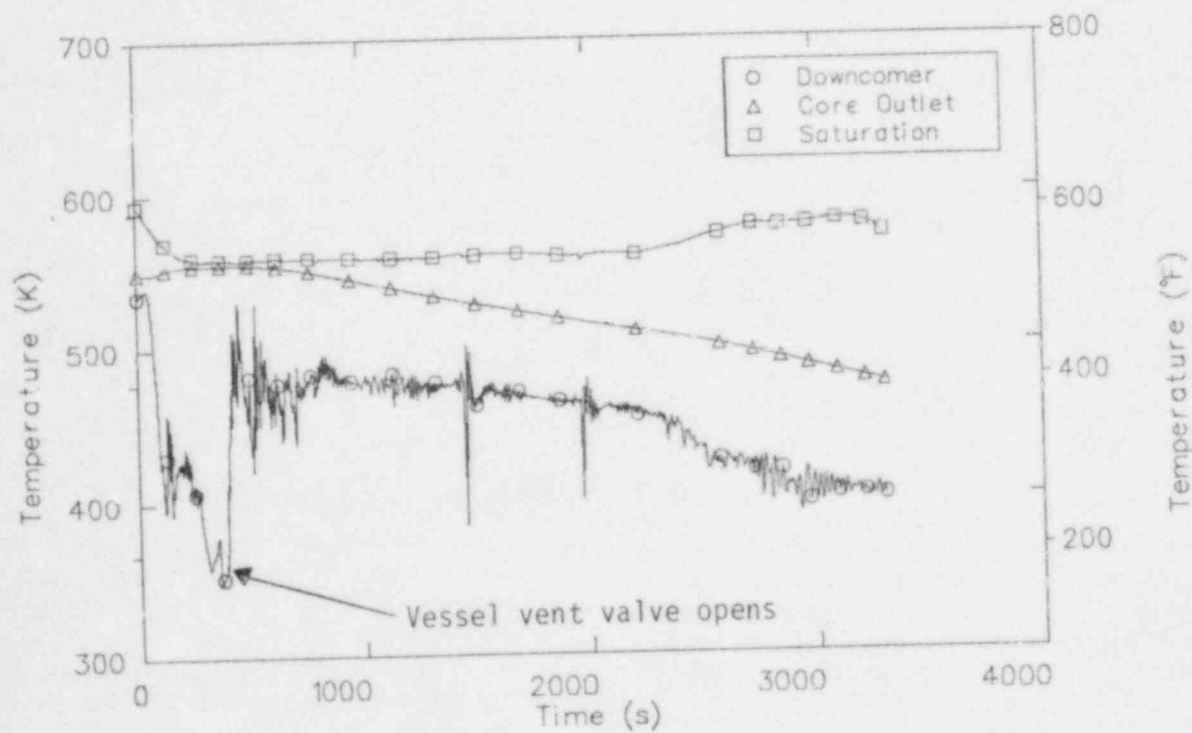


Figure 12. Fluid temperatures at the top of downcomer and core outlet and saturation temperature for the WORVHVL case.

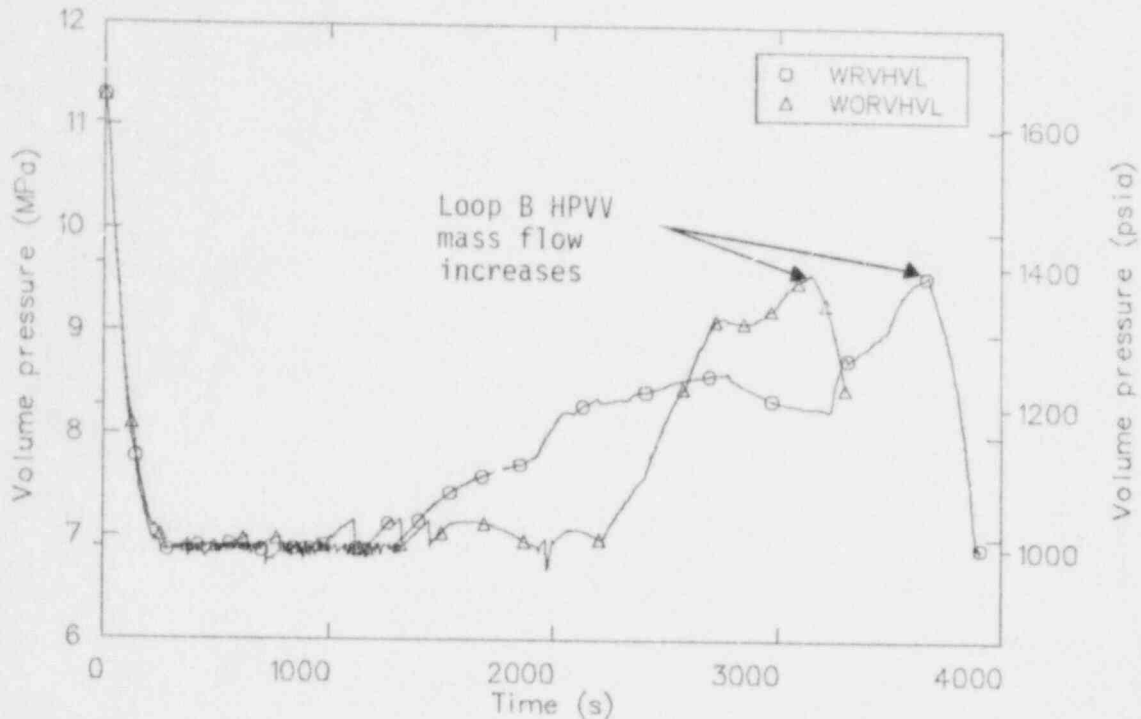


Figure 13. System pressures for the WRVHVL and WORVHVL cases.

region proved to be the principal region dominating pressure increases in both simulations. Pressure increases occurred after a significant fraction of the steam was condensed out of the bubble mixture. Near the end of the simulations, the pressures had reached maximum values of 9.6 MPa (1390 psia) before turning over.

Figure 14 presents the calculated HPV mass flow rates for the WRVHVL and WORVHVL cases. The HPVVs are located at the top of the hot leg U-bends. The mass flow rates increased when the U-bend regions became two-phase. These transitions occurred in Loop A at 2200 s and 2485 s and in Loop B at 3424 s and 2951 s for the WRVHVL and WORVHVL calculations. The RELAP5/MOD2 critical flow problem briefly described in Section 3 caused the increased Loop B HPVV flow rates and an attendant pressure decrease at 3124 and 3661 s. These flow transitions occurred after Loop B was refilled and consequently did not affect the results of the refill analyses. The Loop A HPVV flows did not behave similarly, because the HPVV modeling was changed prior to the transition from single-phase vapor flows to two-phase conditions.

Results of Lowered-Loop Analysis

Noncondensable gas removal from the upper head

of a reactor vessel following recovery of natural circulation was analyzed using the results of a RELAP5/MOD2 calculation. The analysis simulated operation of HPVVs and selected operating procedures. The operating procedures used the HPI system, the pressurizer PORV, and the pressurizer heaters. The turbine bypass valves controlled the secondary system pressure. Emergency feedwater controlled the steam generator levels.

Figure 15 shows the HPVV flow rate responses. The HPVVs are located at the top of the hot leg U-bends. The rated flow through the HPVVs was 1.3 kg/s (3 lbm/s) single-phase vapor at 15.65 MPa (2270 psia). This corresponds to 10% of the pressurizer PORV capacity. The initial flow rates were higher than the rated flow, because the flow was liquid instead of vapor.

The HPVV flow rates were generally less than 6.8 kg/s (15 lbm/s). Errors in extrapolating water properties from the upstream volume to the HPVV junction caused the flow spikes before 1000 s. These flow spikes did not affect the analysis, because noncondensable gas was not removed during this period. The HPVV flow responses became smoother after the U-bends became two-phase at 1000 s.

Figure 16 shows the hot leg U-bend void fraction responses. Continued primary system depressurization

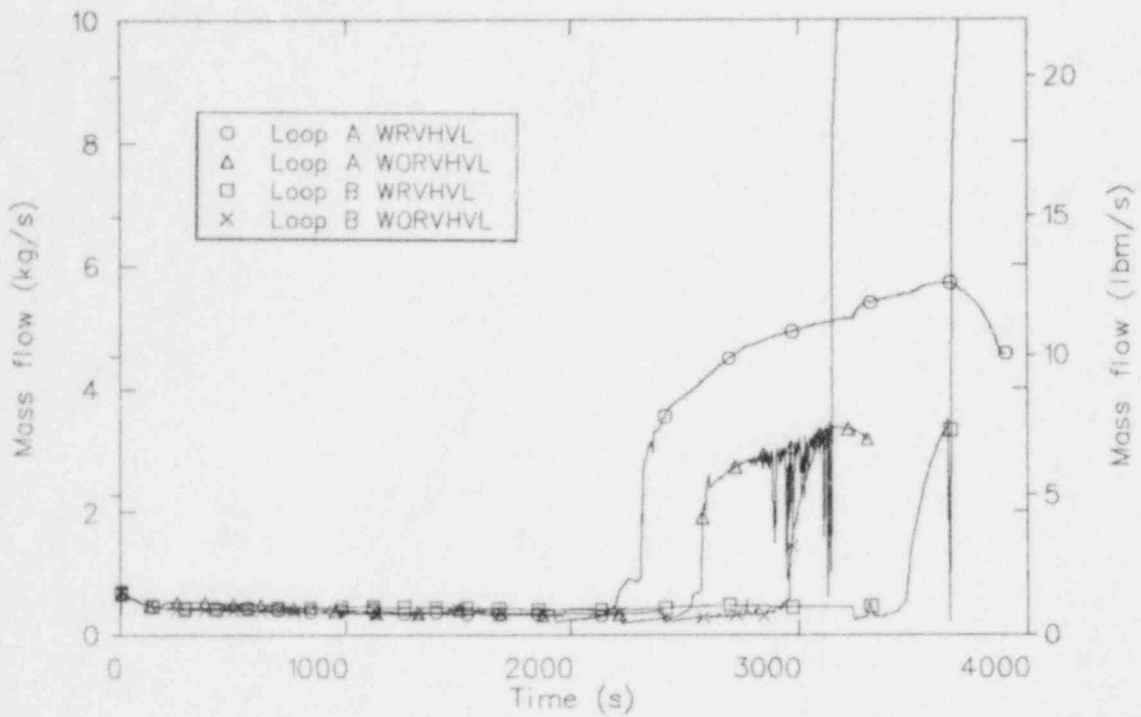


Figure 14. HPVV mass flow rates for the WRVHVL and WORVHVL cases.

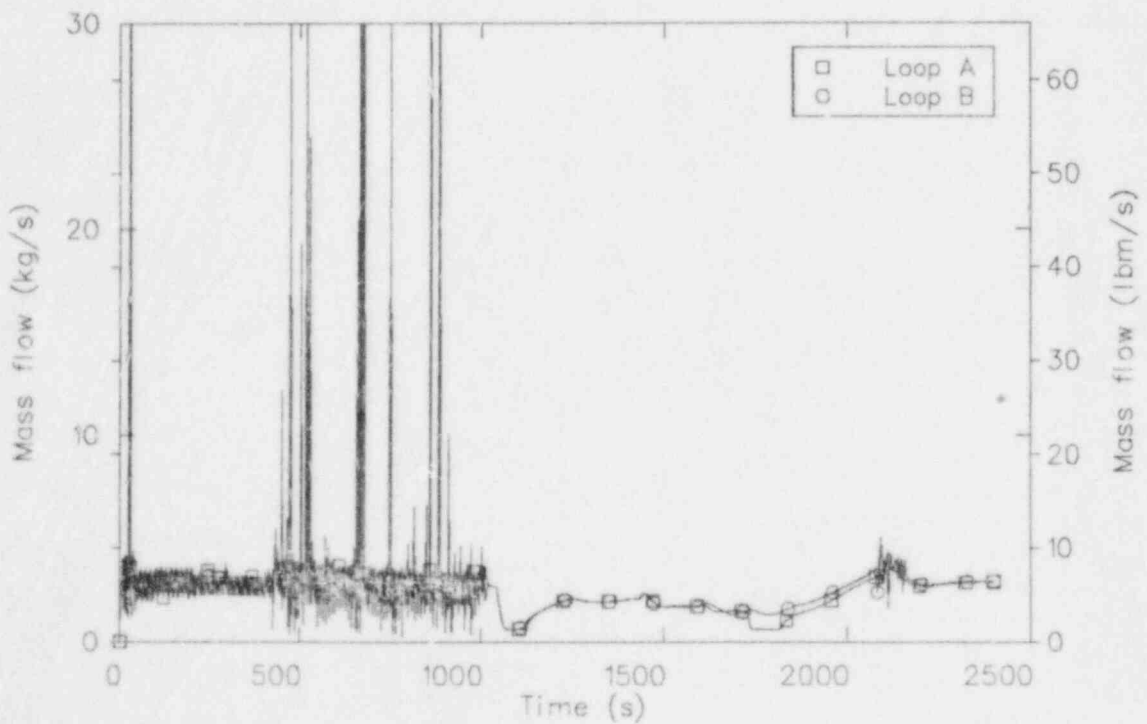


Figure 15. Lowered-loop HPVV mass flow rates.

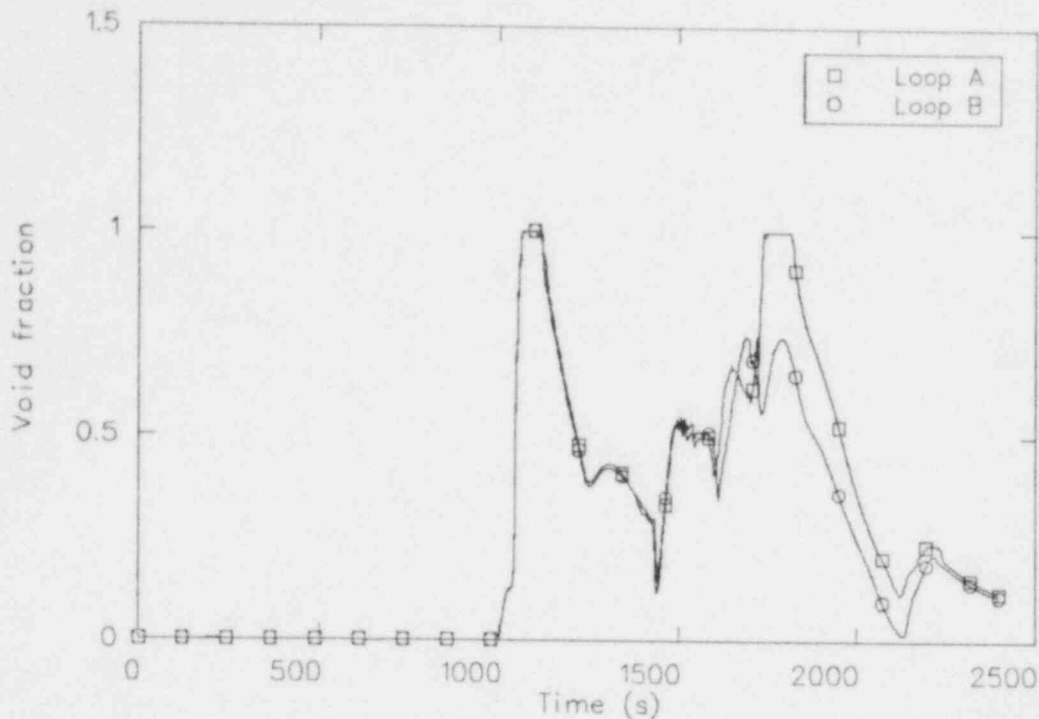


Figure 16. Lowered-loop hot leg U-bend void fractions.

expanded the noncondensable bubble in the vessel upper head down to the vessel outlet, as shown in Figure 17. Natural circulation moved part of the bubble into the hot legs, which caused the rapid void fraction increases at 1000, 1400 and 1620 s.

Figure 18 shows the hot leg U-bend mass flow rate responses. The movement of the noncondensable bubble from the reactor vessel to the U-bends caused the flow increases at 1000, 1400 and 1620 s. The buoyancy of the bubble pushed the water in the hot legs up to the U-bends. The bubble rose to the top of the U-bends and temporarily stopped natural circulation. Without natural circulation, additional noncondensable gas could not be removed from the vessel. The bubble in the top of the U-bends was subsequently removed by the HPVVs. The density head in the steam generator tube bundles and the removal of the U-bend bubbles caused the resumption of natural circulation.

Figure 19 shows the desired primary system pressure control used in the RELAP5/MOD2 model and the calculated primary system pressure response. The primary system pressure decreased to 11.7 MPa (1700 psia) by 1120 s, which was faster than the desired rate. The pressurizer heaters were at full power during this period. Nevertheless, they were not able to overcome the pressure-reducing effects of the

opened HPVVs and the primary-to-secondary heat transfer. The PORV was closed during this period and consequently did not contribute to the primary system depressurization.

The primary system pressure increased between 1120 and 1200 s, because primary-to-secondary heat transfer was retarded by the nearly stagnant loop conditions. The stagnant conditions caused the coolant temperatures in the core and hot legs to increase. The increasing temperatures subsequently caused coolant expansion and thereby repressurized the primary system as the vapor regions were compressed.

The rate of primary system depressurization decreased at 1450 s as the bubble in the vessel upper head expanded into the hot legs. This retarded natural circulation, thereby reducing the primary-to-secondary heat transfer rate from 70 to 35 MW. This reduction in the rate of depressurization indicates the relative effects of HPVV flow and primary system cooldown on the primary system depressurization rate.

The depressurization rate from 1450 to 1720 s was essentially constant. The depressurization rate continued to be less than the initial rate, because the primary system mass flow rates after 1100 s were less than those during the first 1100 s. This resulted in reduced rates of primary-to-secondary heat transfer.

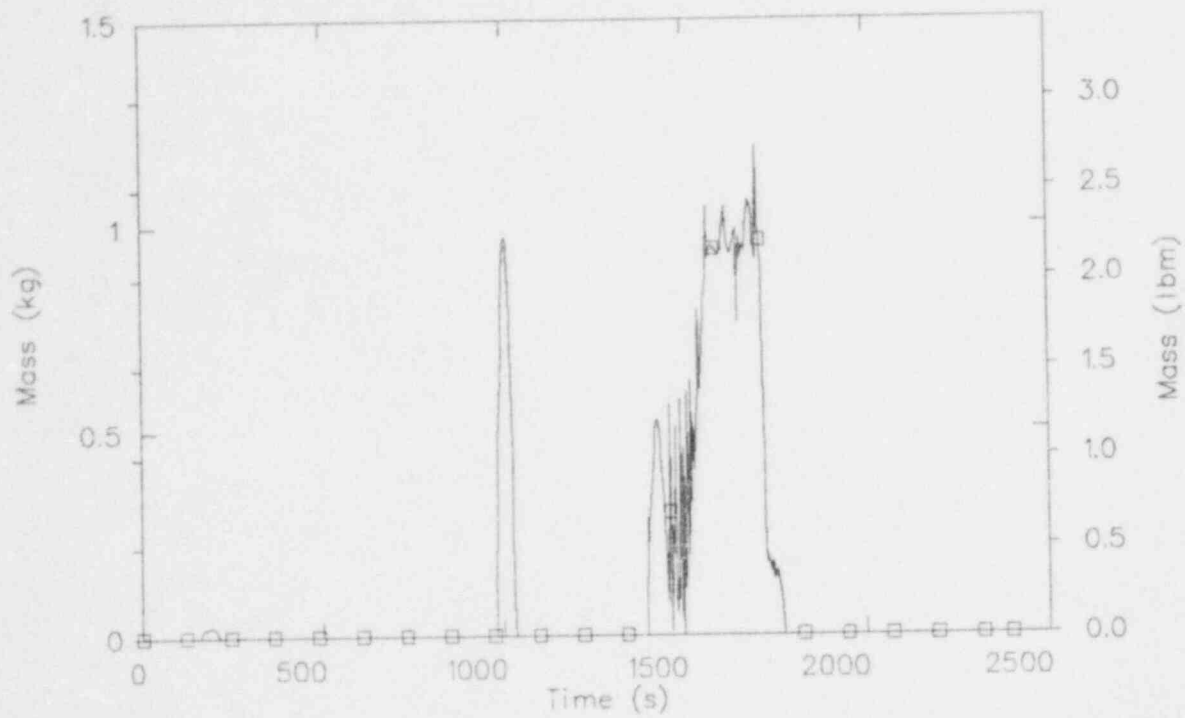


Figure 17. Noncondensable mass at the lowered-loop vessel outlet.

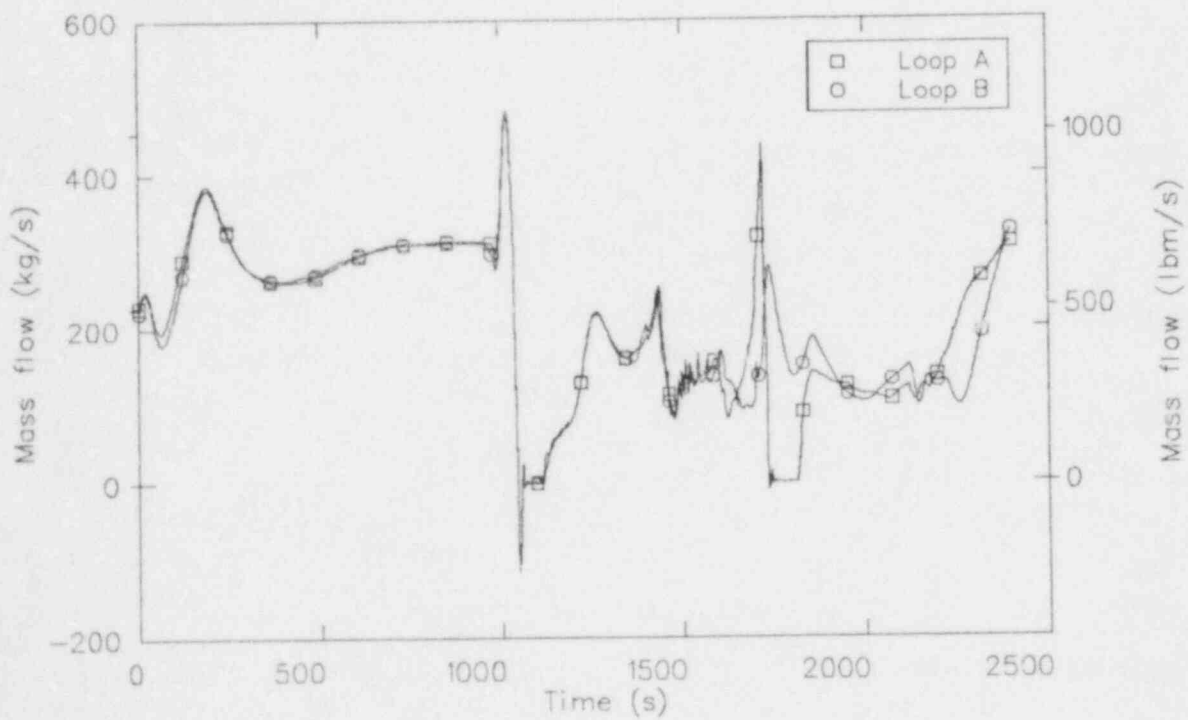


Figure 18. Lowered-loop hot leg U-bend mass flow rates.

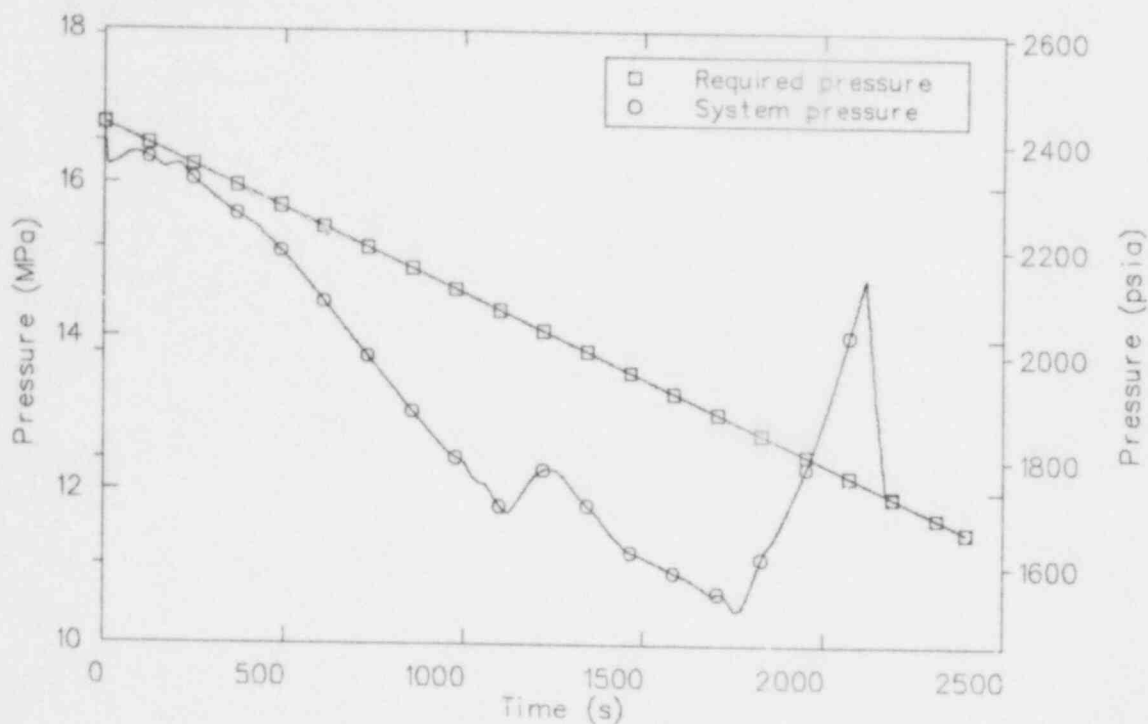


Figure 19. Desired and calculated lowered-loop primary system pressures.

Figure 20 compares the RELAP5/MOD2 saturation temperature with the Loop A fluid temperature. The difference between the two temperatures was used as an indication of liquid subcooling. HPI initiation at 1760 s on low subcooling caused the rapid pressure increase starting at 1800 s. A small noncondensable bubble in the pressurizer decreased the water vapor partial pressure. This lowered the RELAP5/MOD2 saturation temperature and the corresponding indicated subcooling in the Loop A hot leg. The decreased subcooling initiated HPI. This would not be done in a prototype plant, because the saturation temperature is obtained as a function of the indicated pressure and not the water vapor partial pressure as used in the RELAP5/MOD2 model.

HPI was terminated at 2115 s when the subcooling reached 55.6 K (100°F). The pressure was higher than the desired pressure when HPI was isolated. Recovery of adequate subcooling in conjunction with the higher pressure opened the pressurizer PORV for the first time in the calculation, as shown in Figure 21. The opened PORV decreased the calculated pressure back to the desired pressure by 2175 s. The PORV and pressurizer heaters maintained the desired rate of pressure decrease for the remainder of the calculation.

The use of HPI for primary system pressure recovery appears to be more effective than using only the

pressurizer heaters. This conclusion is based on the primary system pressure responses before and after HPI was initiated at 1760 s. The HPI recovered the primary system pressure in approximately 200 s, whereas the heaters could not. The rate of pressure recovery depends on the primary system pressure, since HPI flow rate increases as the primary system pressure decreases. The pressurizer heaters could not maintain the desired primary system pressure earlier in the analysis, because the primary-to-secondary heat transfer rate was significantly higher.

Figure 22 shows the fraction of noncondensable gas removed from the primary system. The rapid rates of removal occurred during the periods when the bubbles collected at the top of the hot leg U-bends and the U-bends were voided. The single-phase HPVV volumetric flow rates were approximately three times greater than the two-phase flow rates. Consequently, when the U-bend void fractions decreased to less than 1.0, the HPVV volumetric flows decreased. These flow responses governed the noncondensable gas removal rates shown in Figure 22.

The HPVVs removed approximately 20% of the noncondensable inventory during the last 1400 s of the calculation. Seven percent of the noncondensable gas was removed during the first period of loop stagnation. The other 13% was removed at a relatively

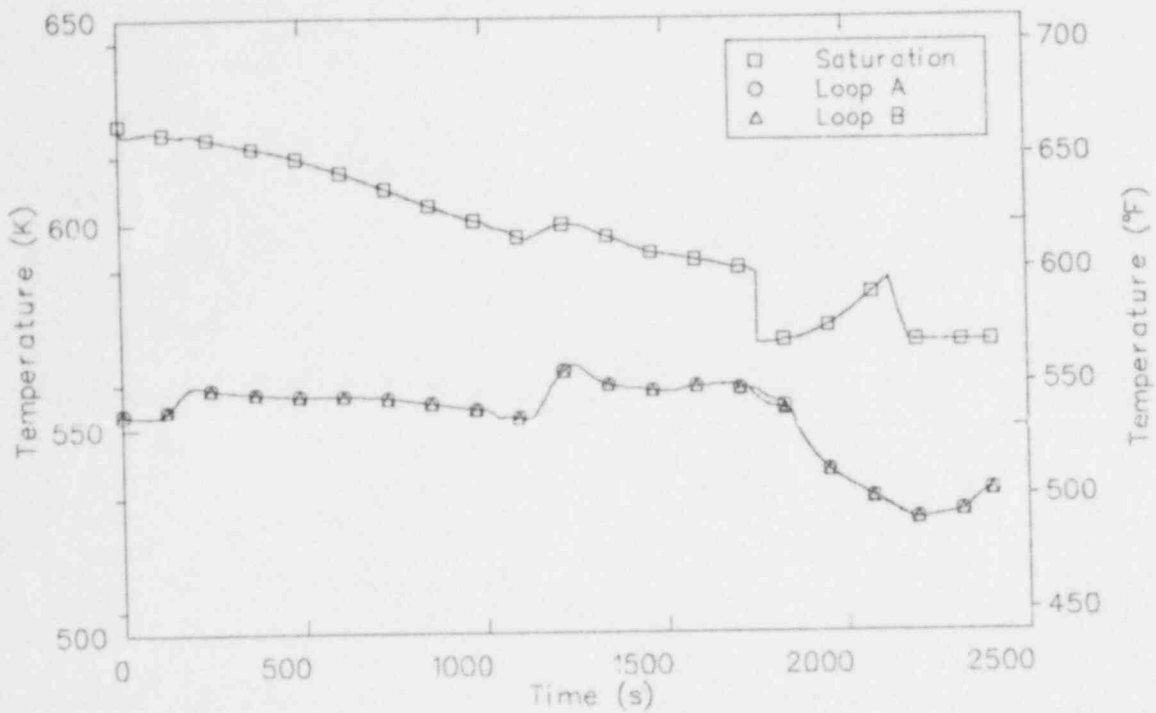


Figure 20. Lowered-loop primary system saturation temperature and hot leg liquid temperatures.

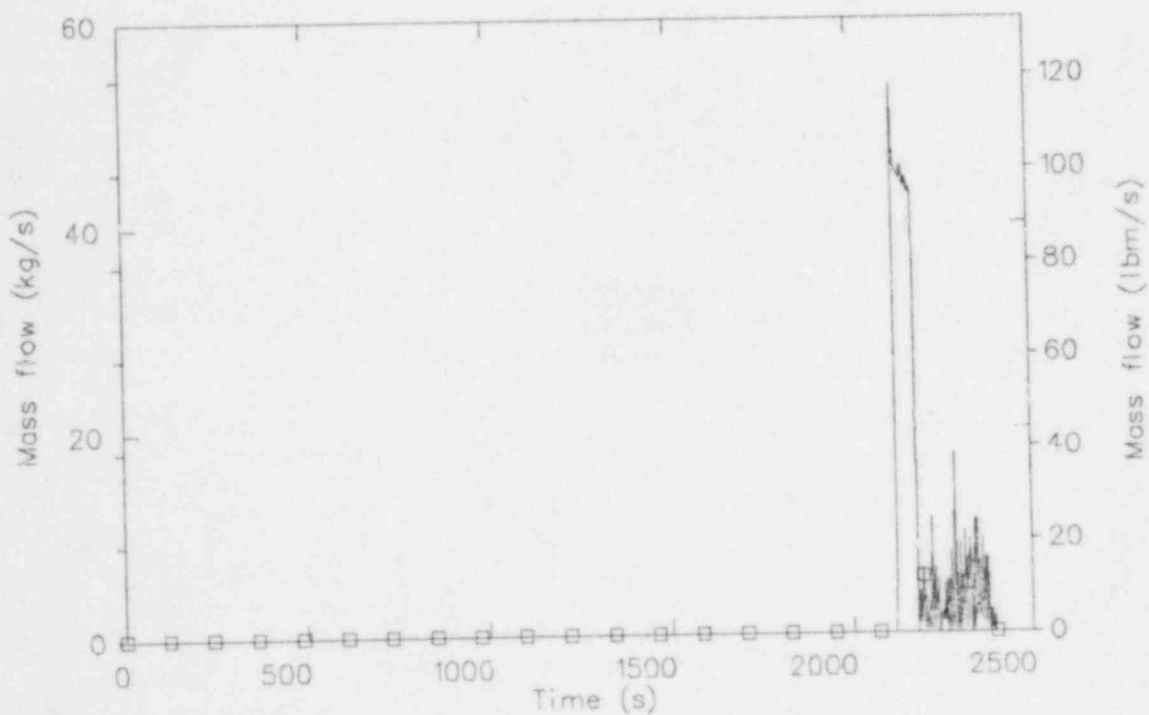


Figure 21. Lowered-loop pressurizer PORV mass flow rate.

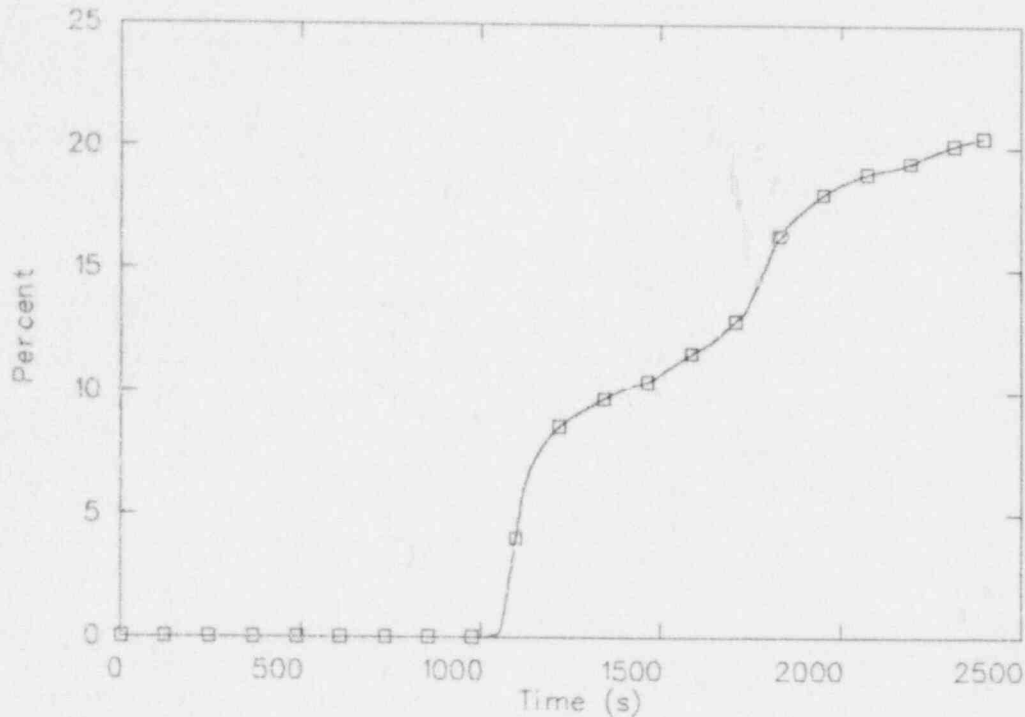


Figure 22. Fraction of initial noncondensable gas removed from the lowered-loop primary system.

constant rate of 1% every 100 s. Given this removal rate, 59% of the noncondensable gas could be removed by the time of low pressure injection initiation at 6900 s.

Figure 23 shows the noncondensable mass inventory in the reactor vessel upper plenum. The mass increased during the first 1000 s as the primary system depressurized and the gas expanded from the vessel upper head into the upper plenum. The hot leg flow surge at 1000 s caused the rapid decrease in bubble mass. HPI began refilling the reactor vessel at 1760 s and forced the noncondensable bubble back into the vessel upper head. This effectively delayed further bubble expansion into the reactor vessel outlet until HPI was isolated at 2115 s.

The opened PORV caused the bubble to resume expansion into the vessel upper plenum. The calculation

was stopped before the bubble expanded back to the vessel outlets. The rate of bubble expansion was comparable to rates calculated during other periods of bubble expansion. This indicates that the input control rate of depressurization appears to be adequate for noncondensable gas removal.

Figure 24 shows the fuel rod cladding surface temperatures at the six core axial elevations. The temperature increases at 1000 s were the result of loop stagnation. The accelerated temperature decreases from 1775 s to 2130 s were caused by HPI flow into the reactor vessel. The maximum cladding surface temperature was 570 K (568 °F) at 1150 s. This temperature was 30 K (54 °F) below the saturation temperature and was less than the full-power operating temperature.

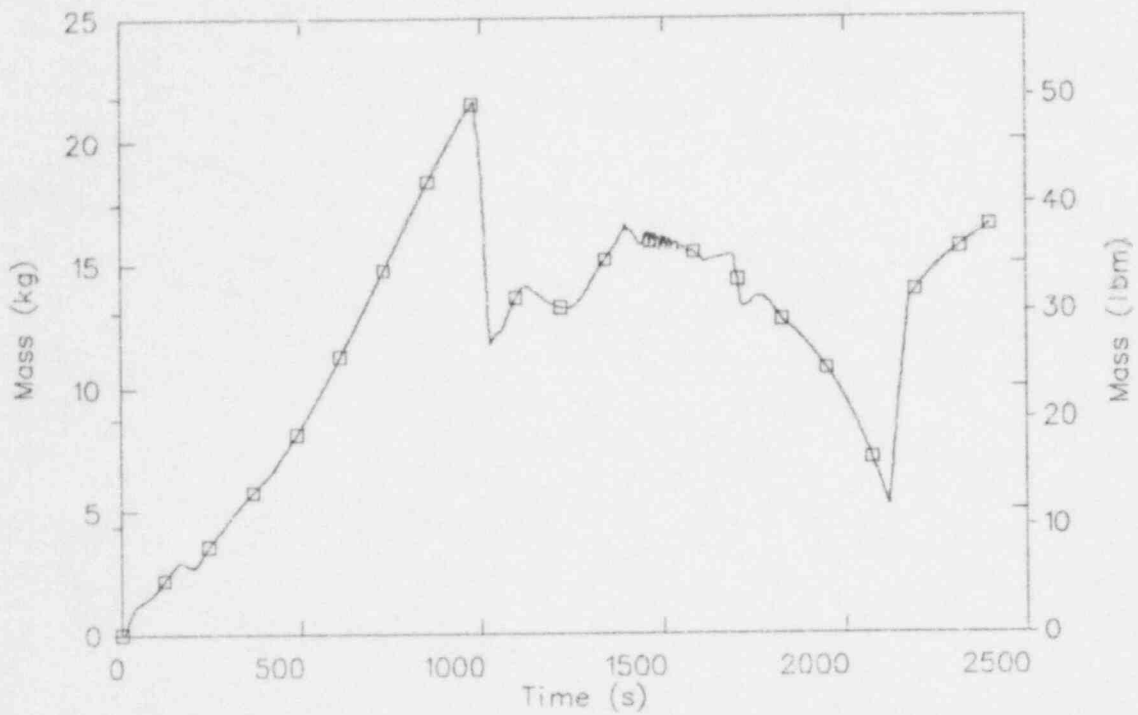


Figure 23. Noncondensable mass in the lowered-loop vessel upper plenum.

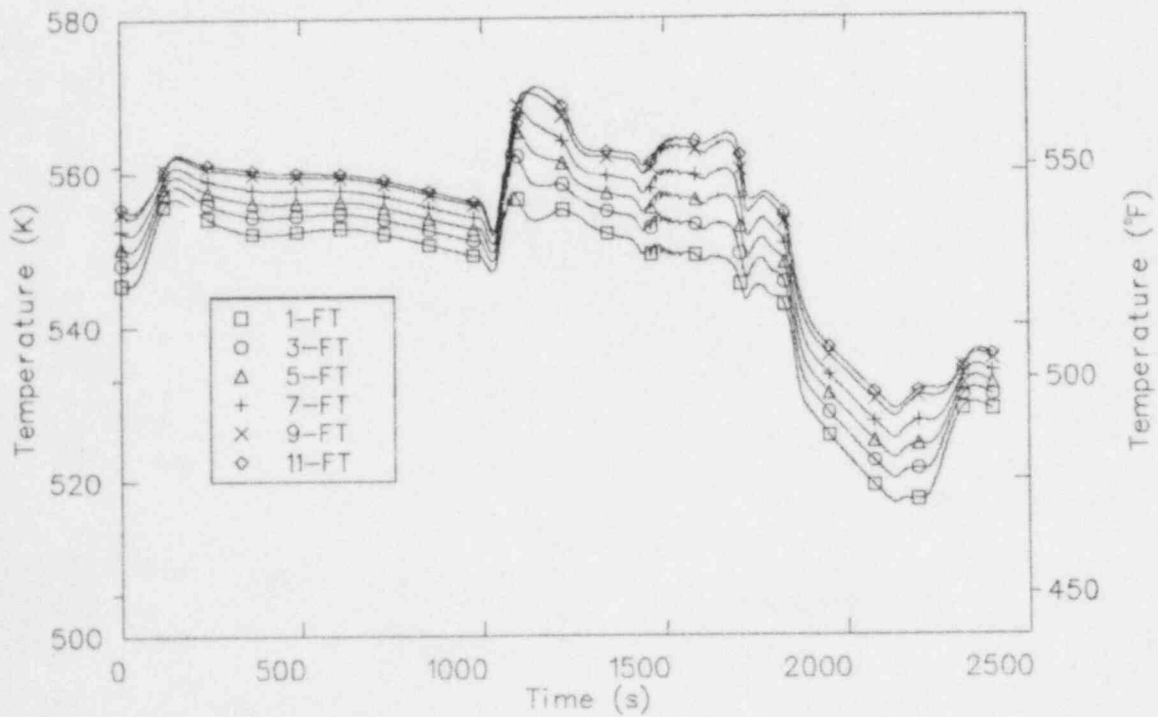


Figure 24. Lowered-loop fuel rod cladding surface temperatures at six axial elevations.

CONCLUSIONS

Conclusions regarding the raised-loop and lowered-loop analyses are presented in the following sections.

Raised-Loop Primary System Refill

Analyses of a raised-loop primary system refill with and without a RVHVL were performed. Each RELAP5/MOD2 calculation was initiated from the same initial conditions. The conditions simulated a plant 2 h after a severe core damage accident, accompanied by significant amounts of noncondensable gas in the primary system. The principal conclusions drawn from the raised-loop refill analyses are as follows:

It was possible to refill the primary system using the HPI system and bridge the tops of the steam generator hot leg U-bends. The use of the RVHVL did not prevent the filling of Loop B but delayed refill by approximately 520 s relative to the WORVHVL case. The RVHVL was connected to the loop without the pressurizer to ensure conservative refill times. The Davis-Besse licensee intends to connect the RVHVL to the loop with the pressurizer. Connecting the RVHVL to the loop without the pressurizer can delay the refilling of the primary loops relative to the time required using the intended design, but the amount of delay has not been quantified.

The HPVVs effectively vented noncondensable gas trapped in the primary system.

The modulation of the pressurizer PORV in conjunction with the HPVVs proved to be effective in maintaining the primary system pressure below the HPI shutoff head.

Refill of the up sides and down sides of the steam generator hot leg U-bends is a necessary but not a sufficient condition for beginning core decay heat removal via natural circulation. An adequate differential pressure induced by density gradients between the vessel and loops must exist to drive loop natural circulation.

Both simulations demonstrated that if HPI is operated at its maximum rate, after loop refilling the net density head provided by core decay heat will not be sufficient to drive loop natural circulation. If HPI is isolated after the loops are refilled, core decay energy will eventually heat up the primary system and thereby establish density gradients sufficient to drive loop natural circulation. Additional analysis is required to develop operating strategies for throttling HPI to ensure recovery of natural circulation in a timely manner.

The HPI flow rate was not regulated to maintain the downcomer temperature within typical recommended

limits. The purpose of this task was to investigate the effect of the RVHVL on primary system refill behavior. System refill times would be increased if HPI were throttled to maintain recommended downcomer temperatures. Throttling HPI below its maximum rate prior to refilling the loops would also ensure a sufficient density gradient to maintain natural circulation after system refill.

Lowered-Loop Noncondensable Gas Removal

The lowered-loop noncondensable gas removal analysis was performed using a RELAP5/MOD2 model of the Oconee-1 plant. The initial conditions simulated a plant 2 h after a severe core damage accident, accompanied by significant amounts of noncondensable gas in the reactor vessel upper head. The principal conclusions drawn from the simulation of the noncondensable gas removal analysis are as follows:

Approximately 20% of the noncondensable inventory was removed during the last 1400 s of the calculation. Seven percent was initially removed as the bubble expanded to the vessel outlet. The other 13% was removed at a relatively constant rate of 1% per 100 s. The sequence of events leading to noncondensable gas removal appears to be cyclic, indicating a high probability of additional gas removal at the same rate. Potentially, an estimated 59% of the total inventory could be removed in 6900 s (the estimated time required to depressurize to the low pressure injection pump shutoff head).

Loop stagnation was predicted for periods of approximately 100 s. In both cases, natural circulation was established without assistance from the control systems. The periods were brief enough that it is doubtful that a plant operator would respond before the plant recovered itself. Nevertheless, the plant operator could recover natural circulation using HPI. Isolation of the HPVVs is not recommended, because the bubble at the top of the hot leg U-bends must be removed to recover natural circulation.

The pressurizer heaters could not maintain the desired primary system depressurization rate with the HPVVs open, and there was a significant primary-to-secondary heat transfer rate. This response could possibly be used by the operator as an indication of voiding in the hot leg U-bends. HPI was able to recover the primary system pressure, but delayed the rate of noncondensable gas removal.

The rate of bubble expansion into the reactor vessel outlet plenum appears to be adequate at the depressurization rate used in this analysis. Higher rates of

depressurization could be achieved, but do not appear to be necessary with respect to noncondensable gas removal from the reactor vessel upper head.

REFERENCES

1. *Clarification of TMI Action Plan Requirements*, NUREG-0737, November 1980.
2. Victor H. Ransom et al, *RELAP5/MOD2 Code Manual, Vols. 1 and 2*, NUREG/CR-4312, EGG-2396, August 1985.
3. C.D. Fletcher et al, *RELAP5 Thermal-Hydraulic Analyses of Pressurized Thermal Shock Sequences for the Oconee-1 Pressurized Water Reactor*, NUREG/CR-3761, June 1984.
4. *Arkansas Nuclear One Unit-1 Emergency Operating Procedures, 1201.01, Rev. 2*, May 4, 1983.

NRC FORM 326 (2-84) NRCM 1102 3201 3202 BIBLIOGRAPHIC DATA SHEET SEE INSTRUCTIONS ON THE REVERSE		U.S. NUCLEAR REGULATORY COMMISSION REPORT NUMBER (Assigned by TIDC and Vol. if any) NUREG/CR-4489 EGG-2436	
2. TITLE AND SUBTITLE VENTING OF NONCONDENSIBLE GAS FROM THE UPPER HEAD OF A B&W REACTOR VESSEL USING HOT LEG U-BEND VALVES		3. LEAVE BLANK	
5. AUTHOR(S) Michael E. Waterman Craig M. Kullberg Philip D. Wheatley		4. DATE REPORT COMPLETED MONTH: March YEAR: 1986	
7. PERFORMING ORGANIZATION NAME AND MAILING ADDRESS (Include Zip Code) EG&G Idaho, Inc. Idaho Falls, Idaho 83415		6. DATE REPORT ISSUED MONTH: March YEAR: 1986	
10. SPONSORING ORGANIZATION NAME AND MAILING ADDRESS (Include Zip Code) EG&G Idaho, Inc. Idaho Falls, Idaho 83415		8. PROJECT/TASK/WORK UNIT NUMBER	
12. SUPPLEMENTARY NOTES		9. FIN OR GRANT NUMBER A6825	
13. ABSTRACT (200 words or less)		11a. TYPE OF REPORT Research	
14. DOCUMENT ANALYSIS - KEYWORDS DESCRIPTORS RELAP5/MOD2, vent valves		15. AVAILABILITY STATEMENT	
5. IDENTIFIERS-OPEN ENDED TERMS		16. SECURITY CLASSIFICATION (This paper) Unc1 (This report) Unc1	
		17. NUMBER OF PAGES 37	
		18. PRICE	

This report describes RELAP5/MOD2 thermal-hydraulic analyses of noncondensable gas removal from Babcock and Wilcox (B&W) reactor systems before and during natural circulation conditions following a severe core damage accident. Hot leg U-bend vent valves were modeled as the principal noncondensable venting pathway. The analyses will assist the NRC in determining whether three B&W plants should receive permanent exemptions from a reactor vessel upper head vent requirement.

The raised-loop plant analysis determined the effect of a reactor vessel upper head vent line on plant refill and recovery of natural circulation and showed that the vent line should be connected to the loop with the pressurizer. The lowered-loop plant analysis investigated the removal of noncondensable gas during natural circulation and showed that 59% of the original inventory could be removed in ~6900 s with a removal rate of ~1% per 100 s. In both analyses, significant amounts of noncondensable gas were removed. Additionally, no fuel rod cladding temperature increases were predicted during the periods of loop stagnation.

14. DOCUMENT ANALYSIS - KEYWORDS DESCRIPTORS RELAP5/MOD2, vent valves		15. AVAILABILITY STATEMENT	
5. IDENTIFIERS-OPEN ENDED TERMS		16. SECURITY CLASSIFICATION (This paper) Unc1 (This report) Unc1	
		17. NUMBER OF PAGES 37	
		18. PRICE	



UNITED STATES
NUCLEAR REGULATORY COMMISSION
Washington, D.C. 20555

April 30, 1986

ERRATA SHEET

Report Number: NUREG/CR-4489
EGG-2436

Report Title: Venting of Noncondensable Gas From the Upper Head
of a B&W Reactor Vessel Using Hot Leg U-Bend Vent
Valves

Prepared by: Idaho National Engineering Laboratory, EG&G Idaho

Date Published: March 1986

Instructions: Report was printed with an incorrect NUREG/CR
identification number.

DELETE: NUREG/CR-4489

REPLACE WITH: NUREG/CR-4488

Division of Technical Information
and
Document Control

120555078877 1 1AN1R4
US NRC
ADM-DIV OF TIDC
POLICY & PUB MGT BR-PDR NUREG
W-501
WASHINGTON DC 20555

EG&G Idaho
P.O. Box 1625
Idaho Falls, Idaho
83415